2016

# Characterization and Modeling of Sediment Settling, Consolidation and Suspension to Optimize the Retention Rate of Sediment Diversions for Coastal Restoration

Xiaoyu Sha
*Louisiana State University and Agricultural and Mechanical College*

# CHARACTERIZATION AND MODELING OF SEDIMENT SETTLING, CONSOLIDATION, AND SUSPENSION TO OPTIMIZE THE RETENTION RATE OF SEDIMENT DIVERSIONS FOR COASTAL RESTORATION

A Thesis

Submitted to the Graduate Faculty of the
Louisiana State University and
Agricultural and Mechanical College
in partial fulfillment of the
requirements for the degree of
Master of Science

in

The Department of Oceanography and Coastal Sciences

by
Xiaoyu Sha
B.S., China University of Petroleum (East China), 2014
August 2016

## ACKNOWLEDGEMENTS

In my life journey, there are several people who have impacts on my choices of directions. Dr. Kevin Xu is one. I would like to express my deepest appreciation to him, who provided me with the precious opportunity, guidance and advice as an invaluable mentor as well as a friend. I am grateful to Dr. Sam Bentley, whose help and encouragement made it possible for me to accomplish the experiments and model tests. Thank you Dr. Kanchan Maiti for allowing me to use your YSI and refractometer. Also thanks to your scientific questions navigated me to pay more attention to the chemical part of my experiments. I would like to specifically thank Dr. Chris Swarzenski for the fieldtrips to the unbelievable pretty marshes; thanks for giving me strength and confidence that I am capable to do a great job.

Thanks to Louisiana Coastal Protection and Restoration Authority (CPRA) Applied Research Program and the Water Institute of the Gulf (TWIG) for supporting and funding this wonderful project (award numbers CPRA-2013-T11-SB02-DR). Thanks to Charlie Sibley and Bill Gibson from Louisiana State University's Coastal Studies Institute's Field Support Group for the best field assistance. Thanks to Howard Callahan and Haifei Yang for helping sample collections in the field. Thanks to everybody in our harmonious Sediment Dynamics Laboratory (SDL) group.

Thanks to the endless love and support from my family and friends. I could not be more grateful to my parents. Thanks for giving me enough freedom and courage to choose my own life, thanks for sharing my happiness and comforting my restless heart, thanks for making me believe the world is gorgeous and waiting for me to explore.

Finally, thanks to fate for everything. Imagine and believe.

## TABLE OF CONTENTS

## ABSTRACT

Many research efforts have been made to the Mississippi coastal restoration, but long-term rheological and sedimentological experiments for sediment erosion, deposition and consolidation in diversion receiving basins are still lacking. Push cores and sediment samples were collected from West Bay, a semi-enclosed bay located on the Mississippi River Delta, and Big Mar pond, a receiving basin of the Caernarvon freshwater diversion from the Mississippi River, Louisiana. A dual-core Gust Erosion Microcosm System was used to measure time-series (0.5, 1, 2, 3, 4, 5, and 6-month after initial settling) erodibility at seven shear stress regimes (0.01-0.60 Pa) using experimental cores prepared with two initial sediment concentrations (60 and 120 kg $m^{-3}$). A 230-cm tall settling column with nine sampling ports was used to measure the consolidation rates for initial sediment concentrations ranging from fluid mud (10 kg $m^{-3}$) to dredge effluent (120 kg $m^{-3}$) in combination with two levels of salinities (1 and 5 PSU). The erodibility of West Bay sediment decreases with increasing time of consolidation. The critical shear stress increases from 0.2 Pa after 2-month of consolidation to 0.45 Pa after 4-month of consolidation. Organic content plays a role on both sediment resuspension and consolidation, particularly for Big Mar sediment. The consolidation rates are inversely and exponentially related to initial sediment concentrations. Sediment in 1 PSU tests generally settles faster than that in 5 PSU tests. A model using a single consolidation rate was improved by adding another exponential coefficient. The improved Sanford (2008) model can better predict the consolidation profile of both rapid early settling and slow self-weight consolidation processes.

# CHAPTER 1. INTRODUCTION

Coastal environments, the habitats for approximately 44% of the world's population within 150 km of coastlines, are mostly retreating (Syvitski et al., 2005). River deltas, one type of major coastal environments, are generally densely populated and heavily farmed. The fate of river deltas is vital to not only nature but also commerce (Day, 2007; Jackson et al., 2001; Syvitski et al., 2009). However, many of the world's large deltas are shrinking rapidly, which motivates the scientists to study the possible reasons and come up with feasible plans to restore the deltas (Stanley and Warne, 1998; Syvitski et al., 2009; Syvitski and Saito, 2007; Wells and Coleman, 1987).

The Mississippi River Delta (MRD, Figure 1) in coastal Louisiana plays an important role to the United States because of its well-known economic, cultural, and natural value (Couvillion et al., 2011; Davies, 1982; Khalil et al., 2011). Meanwhile the MRD is also famous for its high rate of land loss at 42 $km^2$ $yr^{-1}$, with over 4877 $km^2$ loss since 1932 (Couvillion et al., 2011). Louisiana's coastal wetlands, more than ~14,000 $km^2$ of swamp and marsh, are at risk due to such a rapid land loss rate (Khalil et al., 2011).

The severe conversion from land to open water has been attributed to both natural and anthropogenic reasons, offshore sea-level rise, rapid subsidence of Holocene strata, less riverine sediment discharge due to the upstream dam constructions, river channelization, hydrocarbon and ground water withdrawal, among others (Blum and Roberts, 2009; Morton et al., 2006; Reed, 2002; Shea and Karen, 1990; Syvitski and Saito, 2007; Syvitski et al., 2005; Tornqvist, 1996; Tornqvist et al., 2008). In order to maintain the long-term sustainability of the MRD, scientists have been monitoring, comparing and testing existing strategies (Nittrouer et al., 2012; Temmerman and Kirwan, 2015; Tessler et al., 2015; Turner, 1997). Louisiana's Comprehensive

Master Plan for a Sustainable Coast issued by Coastal Protection & Restoration Authority (CPRA) in 2012 is one of the most comprehensive strategies established in Louisiana (CPRA, 2012). One type of the projects promoted by CPRA is river diversion, which aims to supply new sediment for land building by diverting the Mississippi and Atchafalaya Rivers water and sediment into adjacent basins to create new land (Figure 1), is highly debatable about its efficiency. Some studies supported that fluvial sediments are crucial to land building and well-designed diversions can help mitigate wetland loss (Allison and Meselhe, 2010; Day et al., 2007; Kolker et al., 2012; Nittrouer et al., 2012; Smith et al., 2015). Other studies argued that hurricanes contributed the most of the mineral sediments to the coast and only a small fraction of the dredged material transferred from channels can be used for wetland restoration (Craft et al., 2002; Turner et al., 2006). Diverted nutrient-rich river water can also lead to more decomposed soil and threat ecological health of marshes (Swarzenski et al., 2008).

One of our two study sites, West Bay, is the only operational artificial diversion designed for land building purpose in Louisiana (Figure 5A). The other study site, Big Mar, is downstream of Caernarvon freshwater diversion on the lower Mississippi River (Figure 5B, Allison and Meselhe 2010). Another major type of listed project in 2012 Master Plan is marsh creation (Figure 2), which is designed to create new wetlands in open water through sediment dredging and placement. About $20 billion in a total of $50 billion in 2012 Master Plan will be spent on marsh creation in next 50 years (CPRA, 2012). Thus the study of the process and fate of sediment transport, settling, consolidation and resuspension will play key roles in the functioning of restoration strategies.

Xu et al. (2016) reported that silt and clay contents occupy 54.9% and 20.4%, respectively, in a total of 1191 surficial and down-core samples in Louisiana bays and estuaries.

Nittrouer et al. (2008) estimated a yearly bed form sand transport mass equates to 2.5% of the suspended-sediment discharge for the lower Mississippi River. Sand load of the Mississippi river are genrally sequestered before reaching the Gulf of Mexico (GOM) (Allison et al., 2012) but fine sediment is transported further downstream in the system. The characteristics and behavior of fine sediment are crucial to the success of coastal restoration in Lower Mississippi because the major loss of sediment out of the system is on mud, not on sand (Paola et al., 2011).

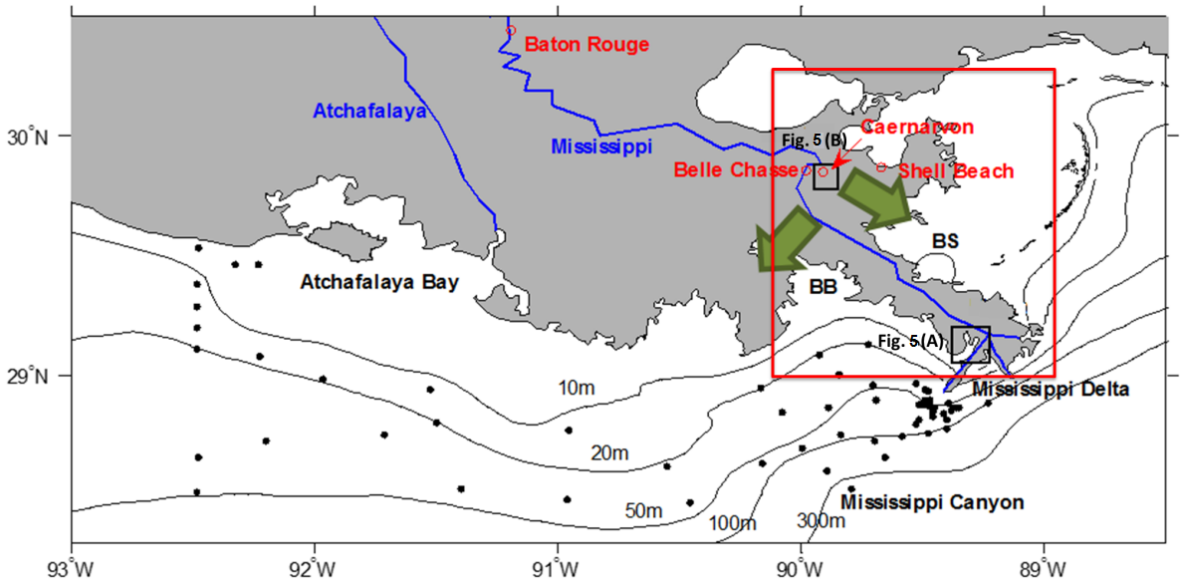


Figure 1. The study area in Louisiana with 10, 20, 50, 100 and 300 m bathymetric contours marked. BS and BB are Breton Sound and Barataria Bay respectively. Green arrows are future large diversions proposed in Louisiana's Master Plan (CPRA 2012). Black dots are erodibility study stations accessed by Xu et al. (2014) on the Louisiana shelf. See Figure 2 for a zoomed-in spatial distribution of Master Plan restoration projects. Two study sites are marked with black boxes, and see Figure 5A, B for details.

Cohesive sediment varies in composition and appearances. The mixture of (saline or brackish) water, clay minerals (mainly illite, chlorite, montmorillonite and kaolinite), a small amount of sand and silt, and organic matter is commonly found in estuarine environments. The 'sticky' nature of cohesive sediment is a result of the chemical forces acting between the plate-like grains with negatively charged faces due to the exposed oxygen atoms in the broken bonds

of the crystal lattice and positively charged edges due to protonation of the broken bonds of the silica tetrahedral (Thorn, 1987). Free cations in surrounding fluid form a layer around the negatively charged grain faces while anions concentrate on the positively charged grain edges. Such an electrical double-layer (EDL, Figure 3) around the clay grain plus a molecular attractive force contributes to the bonding between clay particles, namely cohesion. Absorbed organic materials on clay particles can also help to increase this cohesion (Whitehouse et al., 2000a).

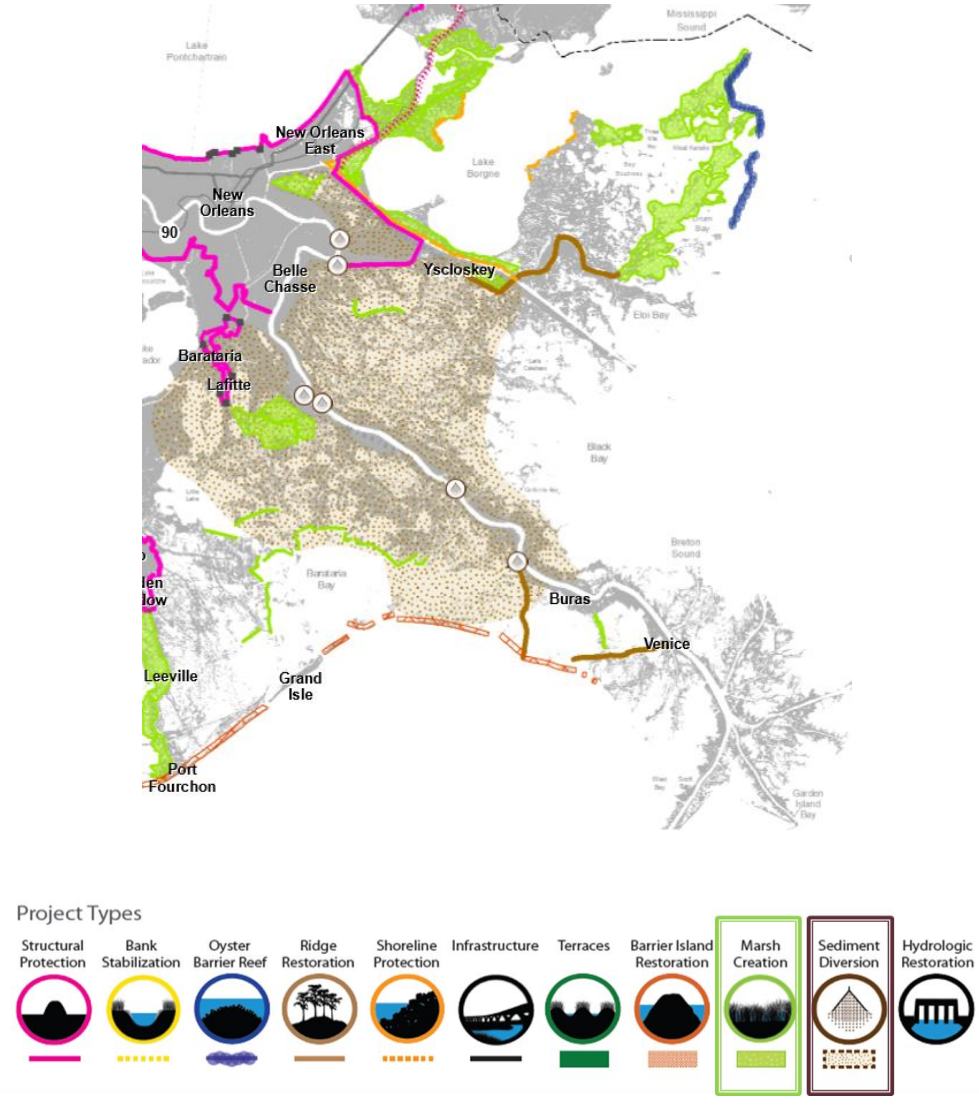


Figure 2. Southeast Coast Louisiana Project Map (CPRA 2012). The brown and green areas indicate sediment diversion and marsh creation respectively.

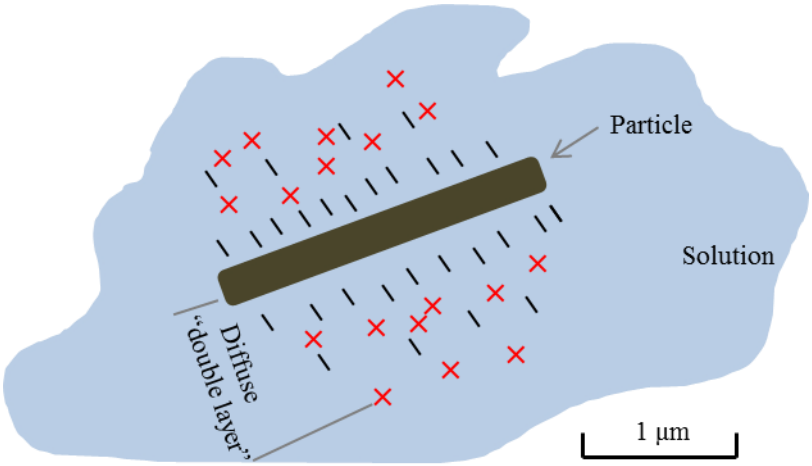


Figure 3. Sketch of particle electrical double-layer in solution. Red crosses mark cations, black short lines mark anions in the solution.

There are four states found in cohesive sediment settling process: suspended sediment, high concentration near bed layer, newly deposited bed and consolidated bed (Figure 4). Difference between surface physical-chemical forces and gravity forces can influence the movement of fine particles (Whitehouse et al., 2000a). When the suspended cohesive sediment particles collide with each other, also called Brownian motion, they stick together to form flocs as a result of cohesion, which is governed by electrostatic forces; after that flocculation takes over (Winterwerp and van Kesteren, 2004). Flocculation is a dominant process of clay minerals in estuaries and deltas because fresh and salt water meets in those places. It strongly influences cohesive sediment transport and distribution. Flocs may have sizes larger than individual particles, and they settle faster than individual particles during flocculation process (Migniot, 1968). Factors like discrete constituent particle sizes, pH and ionic strength of the mud, suspended sediment concentration, mineralogy, organic matter, internal shear and bed shear-stress all contribute to determine the sizes of flocs (Dyer, 1989; Krone, 1972; Whitehouse et al., 2000a; Winterwerp and van Kesteren, 2004).

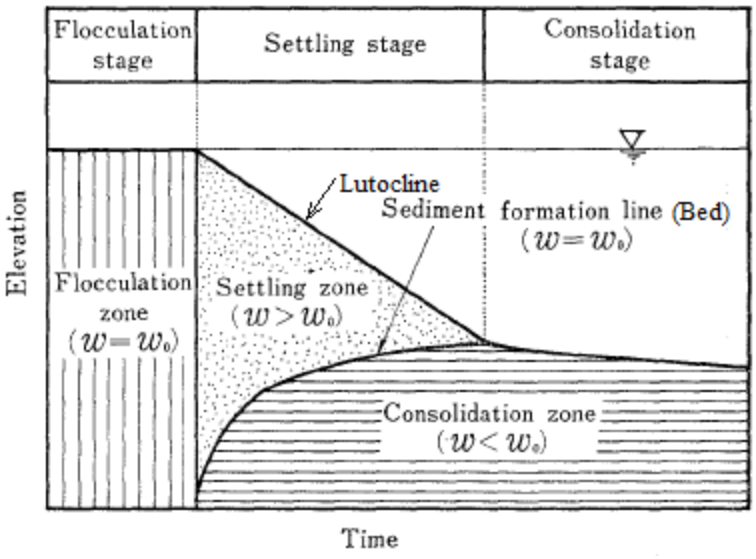


Figure 4. Flocculation, settling and consolidation zones (redrawn from Imai, 1981).

In brackish and saltwater, the double layer and flocculation increase with salinity up to a nominal value (generally 2-3 Practical Salinity Unit, PSU). Salinity beyond this nominal value will not influence the settling velocity very much (Burt, 1986). When the sediment suspension concentration increases, the gap between flocs is similar to the size of the flocs and the flocs start to hinder each other in their settling, hence the hindered settling starts to play a role. In this case, the flocs are supported by the upward fluid flow. Thereafter, if the concentration keeps increasing to become unity, the flocs form a space-filling network and the hindered settling will be overshadowed by self-weight consolidation (Figure 4). In this phase, flocs are supported by particle interactions. The height of the sediment bed surface will decrease during the consolidation process without further sediment input on the bed surface. In addition, microbial mats, films and fecal deposits can smooth the bed surface and decrease the hydraulic stress experienced by the exposed sediment surface (Mariotti and Fagherazzi, 2013; Whitehouse et al., 2000a; Winterwerp and van Kesteren, 2004).

In recent years, several studies have been focused on cohesive sediment processes in the United States. Monthly to bimonthly sediment erodibility measurements have been done in the York River, an estuary of the Chesapeake Bay in East Coast, to evaluate the correlation between solids volume fraction of the mud matrix and bed erodibility (Dickhudt et al., 2011). A cohesive sediment bed model was calibrated with erosion measurements from the York River to examine processes influencing sediment erodibility and water column turbidity with the consideration of the equilibrium state between consolidation and swelling by Rinehimer et al. (2007). In the MRD of northern Gulf of Mexico, Xu et al. (2016) conducted field measurements of the erodibility of bed sediment at West Bay and Big Mar in dry season (November) and calculated wave-induced shear stresses in Louisiana bays. Xu et al. (2014) and Mickey et al. (2015) quantified critical shear stress and eroded mass of >100 sediment cores collected on Louisiana shelf in early spring and late summer seasons.

Lo et al. (2014) collected sediments from Lake Lery, a shallow basin receiving freshwater and sediment from Caernarvon Diversion via Big Mar, and experimentally determined the time dependency of sediment erodibility after one, two and four weeks of settling, as well as consolidation rates for suspended sediments with different initial concentrations. Lo et al. (2014) found that after 1 month of consolidation sediment is still much more erodible than the sediment normally found in Louisiana estuaries and shelf. Although many efforts have been made to the protection and restoration of the Mississippi deltaic coast, long-term (e.g., up to six months) rheological and sedimentological measurements/experiments for diverted sediment erosion, deposition, and consolidation in receiving basins are still lacking. Differing than the study of Lo et al. (2014), this study compared cohesive sediment behavior from a receiving basin which is under strong oceanographic influence (West Bay) with a more landward waterbody (Big Mar).

Two salinity (1and 5 PSU) conditions were used to quantify the settling behavior, instead of just one (5 PSU) being conducted by Lo et al. (2014). The time scale of this study for sediment to consolidate was extended from 1 month to 6 months after initial settling. In addition, laser grain size and organic matter were analyzed to better quantify the properties of sediments used in the experiments.

In this study, the overall goal is to determine the magnitudes and rates of sediment settling and consolidation for fine-grained, cohesive river sediment, and the associated changes in bed erodibility. Specific objectives are: (1) to measure the time-series erodibility of experimental cores over a total of 6-month period using muddy sediment collected from two active Louisiana receiving basins; (2) to characterize the sediment settling and consolidation rates for suspended sediment at concentrations ranges similar to these of fluid mud (Kineke et al., 1996; McAnally et al., 2007) and dredge effluents (Turner, 1996), using 1 and 5 PSU salinity conditions in the laboratory; (3) to test if the correlations between sediment erodibility and consolidation time exist; (4) to quantify the grain size and organic matter of push cores collected in the field and experimental cores 7-month after settling in lab, as well as the grain size of suspended sediment at nine elevations in a settling column; (5) to simulate the sediment settling and consolidation processes by modifying and improving an existing semi-empirical sediment model (Sanford, 2008). Findings of this study can be used to test computational models, inform the design and operation of ongoing and future Louisiana dredging, optimize sediment retention in diversion design receiving basins, and hence potentially help increase land-building capability of various projects in future coastal Louisiana restoration projects.

# CHAPTER 2. MATERIALS AND METHODS

## 2.1 Study Area

Field erodibility measurements and sample collections were performed by Xu et al. (2016) in two receiving basins: West Bay (Figure 5A) and Big Mar (Figure 5B). West Bay is a semi-enclosed bay, located on the MRD, west of the Head of Passes and connected to the GOM. A crevasse in the natural levee system occurred during a rising river flood and led to the fast subaerial growth of West Bay since 1839. By the 1930s, West Bay subdelta reached its maximum size (Figure 6). The subaerial extent reached the maximum of 297 $km^2$ in 1932. Hereafter, deterioration took over at an average rate of 4.1 $km^2$ $y^{-1}$, possibly due to rapid compaction and lack of sediment supply (Wells and Coleman, 1987). A non-gated diversion was operated in West Bay since 2004 for sediment capture purpose (Allison and Meselhe, 2010). It did not build much subaerial land until 2011 river flood, and the growth of a subaqueous delta saved the sediment diversion from being closed.

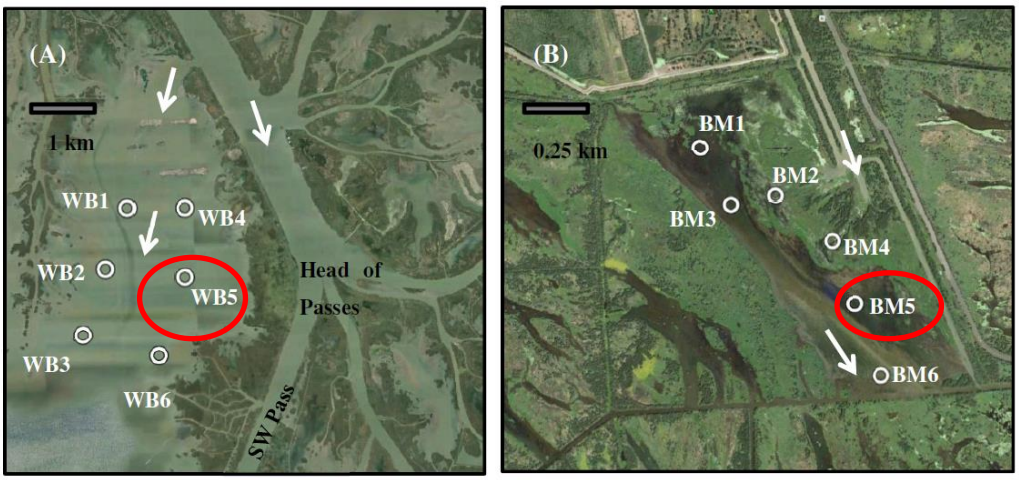


Figure 5. The maps of West Bay (A) and Big Mar (B) study areas. White arrows show the overall flow directions. Push cores and bulk sediment were collected at WB5 station on 19 November 2014. The satellite image for West Bay was collected on 27 January 2015. Push cores and bulk sediment were collected at BM5 station on 7 March 2015. The satellite image was collected on 31 October 2014.

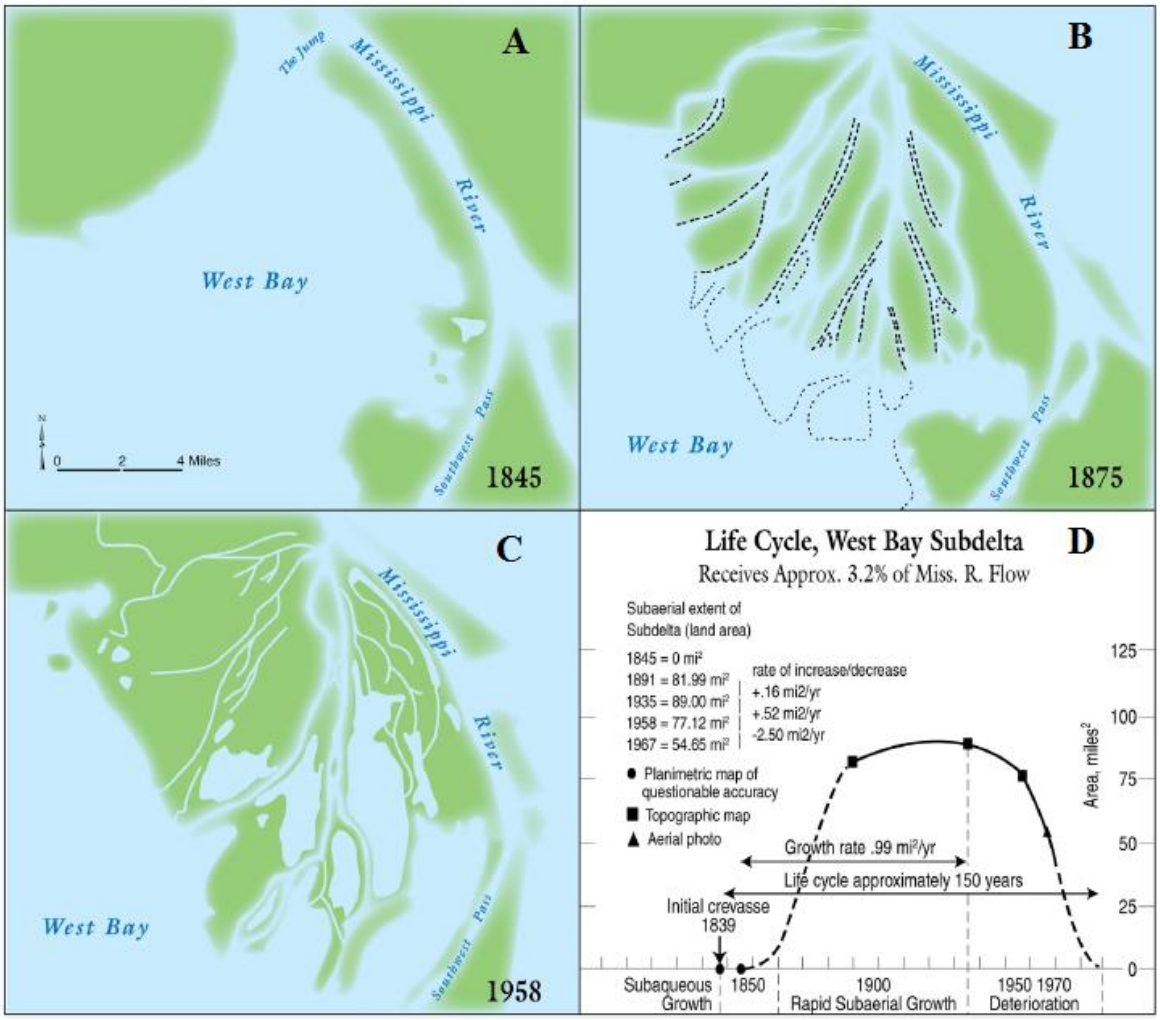


Figure 6. Lifecycle of West Bay subdelta after the crevasse breakthrough in 1839 (Bentley et al. 2016). (A) no obvious land increase, initial stage of subaqueous development; (B) the land area started to increase rapidly since 1875 at an average rate of 2.56 $km^2$/yr; (C) the West Bay subdelta has been deteriorating after its maximum size in 1932; (D) land area changes through the progressive development of the West Bay subdelta.

Big Mar is a large shallow manmade lake caused by a failed agricultural impoundment located south to the small gated freshwater diversion, which has been constructed on the Lower Mississippi River at Caernarvon designed to limit salt water intrusion with minimal sediment capture. Water and sediment passing through the Caernarvon freshwater diversion structure immediately enter Big Mar basin (Allison and Meselhe, 2010; Lane et al., 1999), then flow into Lake Lery and throughout Breton Sound. No significant wetland growth was found within Big

Mar pond until 2004 (Figure 7). Expanded wetland, which was initially floating marsh, acted as sediment trap after Hurricane Katrina in 2005. The wetland growth rate in Big Mar from 2004 to 2011 (0.34 $km^2$/yr) increased about 30 times as from 1998 to 2004 (0.01 $km^2$/yr) (Baker et al., 2011). After 2010, the Big Mar wetland is still growing (Figure 5B and Figure 7D).

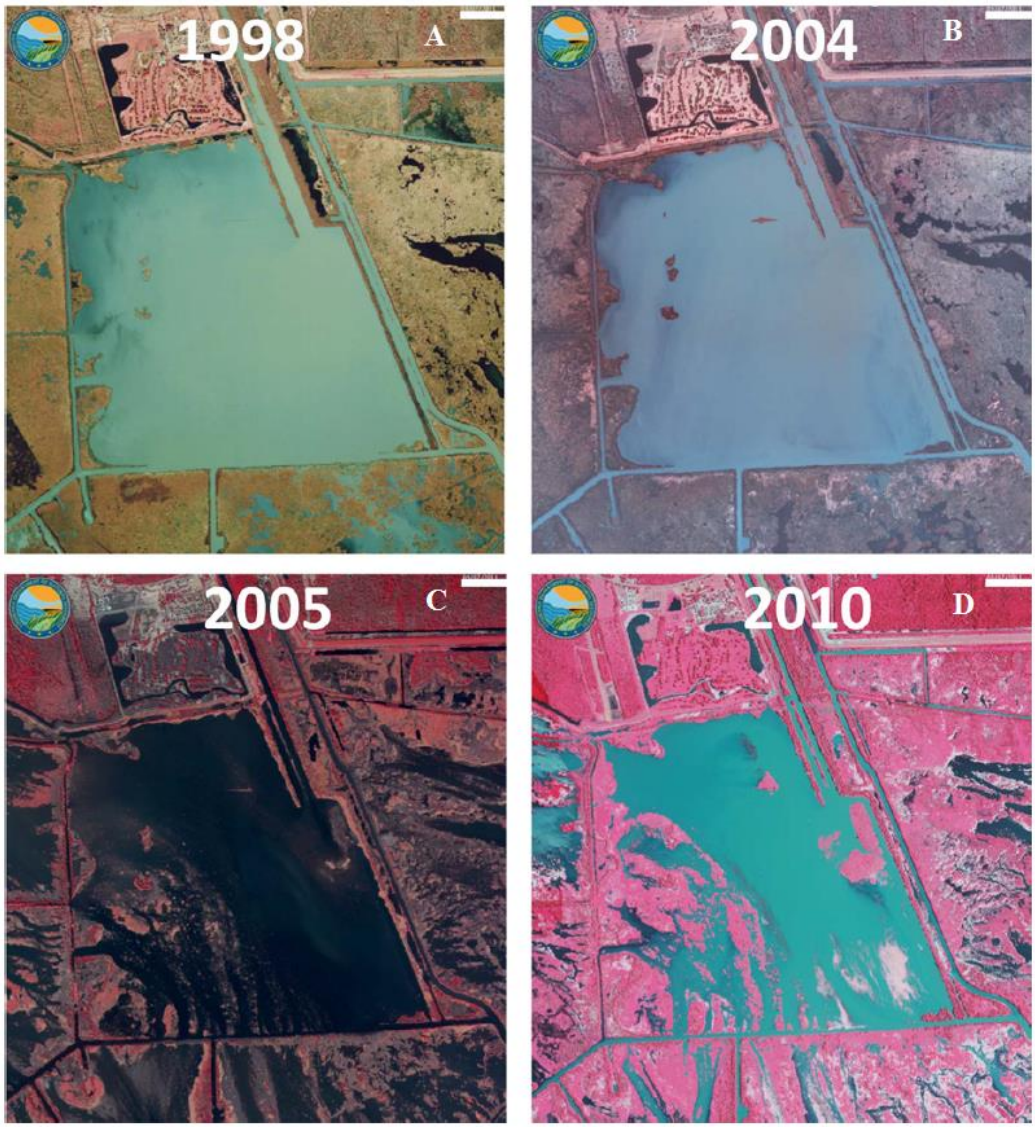


Figure 7. Land change in Big Mar pond from 1998 to 2010. Rapid increase of wetland started after 2004. In 2005 after Hurricane Katrina, some marsh balls were pushed from surrounding marsh into Big Mar pond. About 2.43 $km^2$ of wetland emerged in Big Mar pond from 1998 to 2011, of which 2.35 $km^2$ was gained after 2004 (Lopez et al., 2014). Compare Figure 7D with Figure 5B, the wetland expansion in Big Mar continued after 2010.

## 2.2 Field Work

A shallow-draft Carolina Skiff was used to access West Bay sampling site on November 19th 2014. On March 7th 2015, an airboat was used for Big Mar sampling site because of its shallow water. A meter rod was used to measure water depths on the boat and recorded in Table 1. Stations BM1-BM6 and WB1-WB6 were all studied by Xu et al. (2016), but this study is only focused on stations BM5 and WB5 (Figure 3). WB5 is located near the center of West Bay and BM5 is near the middle of downstream part of the Big Mar pond. Approximately 120 L of bulk sediment was collected at Station WB5 using a Ponar grab sampler which can penetrate about 20 cm deep, and another 120 L of bulk sediment was collected at BM5 using the same device. The bulk sediment was then transported to Sediment Dynamics Laboratory at Louisiana State University (LSU, Baton Rouge, LA, USA) and kept in room temperature for further experiments. In order to simplify the names, "WB" and "BM" will be used hereafter in the results and discussion of this thesis and are actually referred to 120 L bulk sediment collected at two stations. Additional push cores were collected at BM1-BM6 and WB1-WB6 using a push corer, transported to LSU and stored in a cold room for further analyses; only push cores WB5 and BM5 were used in this study.

Table 1. Sampling dates, locations, depths, and organic matter percent of sediments in West Bay and Big Mar.

| Study Site | Fieldtrip Date | Latitude | Longitude | Water Depth (m) | Average Organic Matter Percent of push cores in top 20 cm (%) |
|---|---|---|---|---|---|
| WB5 | 19 November 2014 | 29°8.933'N | 89°17.871'W | 1.22 | 5.56 |
| BM5 | 7 March 2015 | 29°49.818'N | 89°54.190'W | 0.17 | 10.57 |

## 2.3 Sediment Preprocessing

A total of 240 L of bulk sediment collected at WB5 and BM5 were filtered through a 1-mm sieve to remove large organic particulates to prevent interference with apparatus. The sediment was then homogenized and diluted with tap water to concentrations approximately at 10, 40, 60, and 120 kg $m^{-3}$. Three samples were collected from the diluted suspension from the surface, middle and bottom of a 60-L mixing bucket, respectively, for sediment concentration measurements. Four selected concentrations were comparable to the range from natural fluid muds to dredge effluent (Palermo and Thackston, 1988; Turner, 1996). It is well known that the typical Mississippi River sediment concentration is less than 0.4 kg $m^{-3}$ (Nittrouer et al., 2008), which is too low to accumulate at least 10-cm thick of sediment layer required for the erodibility measurements (Lo et al., 2014). All four concentrations were used for consolidation tests. Due to the limited space of the laboratory, only 60 and 120 kg $m^{-3}$suspensions were used to measure erodibility. Artificial sea salt was added to the slurry to prepare the salinities of 1 and 5 PSU for consolidation tests, and only 5 PSU for erodibility experiments. Both salinities are commonly found in Louisiana bays and estuaries. A handheld multi-parameter instrument (YSI 556 MPS) that measures salinity ranges from 0 to 70 PSU was used to determine salinities. This device's accuracy is ±0.1 PSU of reading and its resolution is 0.01 PSU.

## 2.4 Erodibility Measurements

In order to accumulate at least 10-cm thick of sediment layer for erodibility measurements, 45-cm long tubes were connected with 180-cm long tubes using rubber connectors (Figure 8), following the method of Lo et al. (2014). Prepared sediment water mixture was pumped into the tubes using a submersible pump and a garden hose. A total of 14 experimental cores (7 settling durations of 0.5, 1, 2, 3, 4, 5, and 6-month multiplied by 2 initial

sediment concentrations at 60 and 120 kg $m^{-3}$) and 14 additional back-up cores were prepared for West Bay; a total of 28 cores were prepared for Big Mar (Figure 8). About two days after initial settling, the clear water in 180-cm long tubes was drained carefully. The lower short tubes were kept for experiments described below. To avoid confusion, these cores prepared in 45-cm and 180-cm long tubes are all called 'experimental cores'. Some cores were failed during experiment preparation due to leaking problem, but well-preserved cores (clear water-sediment interface, no leaking, no large visible organic mat, and no disturbance) were used for erodibility, organic matter, and grain size analyses.


Figure 8. Picture of sediment tubes for the preparation of experimental cores to be used in Gust Erosion Microcosm System experiments.

A dual-core Gust Erosion Microcosm System (GEMS) was employed to measure time-series erodibility by subjecting experimental cores to well calibrated bed shear stresses (Gust and Muller, 1997).This flow-through system has been widely used to measure fine grained sediment

erodibility over a range of shear stresses both in the field (Dickhudt et al., 2009; Law et al., 2008; Maa et al., 1998; Stevens et al., 2007; Xu et al., 2014) and in the laboratory (Lo et al., 2014). Seven shear stresses (0.01, 0.05, 0.1, 0.2, 0.3, 0.45 and 0.6 Pa) were applied on top of sediment cores by changing spinning rates of two rotating motors inside of erosional heads, which was controlled by a laptop (Figure 9). Water was sucked from source water bucket and transported through the whole system. Each shear stress was kept stable for 20 minutes to capture exponential decay on turbidity and then increased to next higher shear stress level. The 0.01 Pa of shear stress was mainly used for background running purpose. Once the shear stress was increased, more sediment was eroded off the core surface and transported along the tubes, passed through the turbidimeter and trapped in the collection bottles. The sediments and water were filtered through 0.7 μm pore-size pre-weighted glass fiber filters. Then the eroded mass of each step was calculated. The erodibility results were analyzed using formulations of Sanford and Maa (2001):

$$E(m,t) = M(m)[\tau_b(t) - \tau_c(m)] \quad (1)$$

where $E$ is the erosion rate (kg $m^{-2}$ $d^{-1}$); $M$ the locally constant erosion rate parameter (kg $m^{-2}$ $d^{-1}$ $Pa^{-1}$); $\tau_b$ the time-varying bed shear stress; and $\tau_c$ the critical shear stress for erosion assumed to be locally linear in $m$ (sediment bed mass, kg $m^{-2}$). Freshly deposited sediment generally has low values of $\tau_c$ while more consolidated sediment has much higher $\tau_c$ Both $M$ and $\tau_c$ are site-specific. Initial sediment concentrations of 62.82 and 123.95 kg $m^{-3}$ were used for West Bay measurements; 60.11 and 120.03 kg $m^{-3}$ were used for Big Mar measurements. Each experiment was about 3 hours (2 hours plus 1 hour preparation). A total of 30 GEMS experiments have been performed for BM and WB experimental cores.


Figure 9. The GEMS and filtration system (picture taken by R. C. Mickey).

**2.5 Consolidation Tests**

The settling column used in this study is based on the design of US Army Corps of Engineers (US-ACE, Figure 10). The 230-cm tall column was equipped with nine sampling ports at 15 cm intervals. The lowest port was 10 cm above the base of the column and the top one was 160 cm above the base (Figure 10). Four initial suspension concentrations (10, 40, 60 and 120 kg $m^3$) and two salinities (1 and 5 PSU) were used to measure consolidation rates. Suspension was homogenized for 10 min at the beginning of each test. A submersible pump and a garden hose were used to transfer about 60 L of the slurry into the column with a compressor-fed air hose in order to keep the mixture homogenized. Initial elevation was recorded immediately after the introduction. Then a 50 mL centrifuge tube was used to sample each of the nine ports. This entire experiment was performed in room temperature. Both water and sediment-water interface were recorded before and after each sampling event to correct the sampling volume loss. Sampling at

approximately 0, 1, 3, 7, 13, 25 and 49 hours after slurry introduction and was continued until the sediment bed elevation did not change more than 1 cm within 48 hours due to the self-weight consolidation. Each port was flushed with water to clean residual sediments before and after each sampling event.

**2.6 Sanford (2008) Model Modification and Improvement**

The experimental sediment bed elevation data collected in the settling column, hereafter referred to as the experimental data, were used to test the consolidation profile prediction of Sanford (2008) model. Initial and final conditions were defined by initial sediment concentration and height, and equilibrium solids volume fraction at water-sediment interface and asymptotic solids volume fraction at the lowest sampling port during the last sampling event. The solids volume fraction was determined using a method described by Mulsow et al. (1998):

$$\emptyset_s(d) = \emptyset_{s\infty} - (\emptyset_{s\infty} - \emptyset_{s0})e^{-ad} \qquad (2)$$

Where $\emptyset_s(d)$ is the solids volume fraction at depth $d$, $\emptyset_{s0}$ and $\emptyset_{s\infty}$ are the solids volume fraction at the water-sediment interface and at great depth (the lowest sampling port during the last sampling event here), respectively, and $a$ is an empirical exponential coefficient.

Sanford (2008) is a one-dimensional (1D) model using a single exponential consolidation rate. Lo et al. (2014) reported that Sanford (2008) formulation was good in predicting consolidation profile over short timescales (<168 h), but underestimated the self-weight consolidation stage. In this study, the time for sediment needs to enter the self-weight consolidation stage from early settling was determined by the regression analysis of the experimental data. Methods described by Sanford (2008) were used for the early settling stage by adjusting only the first-order consolidation rate $r_c$. In this study another empirical exponential coefficient was added to the Sanford (2008) consolidation profile prediction for the self-weight

consolidation stage. As described in discussion later, the prediction curves are plotted with the experimental data and regression analysis lines.

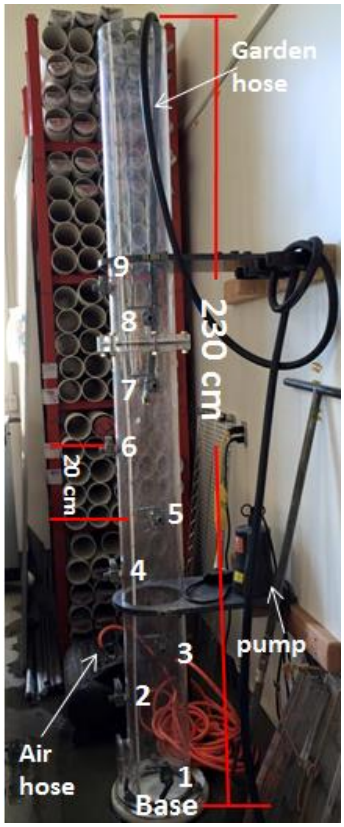


Figure 10. The settling column with nine sampling ports at 15 cm intervals. Each sampling event started with the No. 1 port at the top. The submersible pump, garden hose, compressor-fed air hose and base are marked.

**2.7 Grain Size Analysis**

A Beckman-Coulter laser diffraction particle size analyzer (Figure 11, Model LS 13 320) was employed to measure grain size for subsamples of push cores WB5 and BM5 collected in the field, experimental cores prepared in 50-cm and 200-cm tubes, and slurries collected in the settling column. Two push cores WB5 and BM5 were split into halves at a laboratory in LSU. Because the bulk sediment was collected using grab sampler which can penetrate about 20-cm

deep, for comparison purpose the top 20-cm of the split cores were sliced into 2-cm slices for grain size analysis.

Four experimental cores originally prepared in 50-cm and 200-cm tubes were untouched and then used to measure the surficial grain size distribution. The GEMS sediment cores of West Bay and Big Mar have been resting in the laboratory in room temperature for 12 and 7-month, respectively. A cut-head syringe was used to collect the top 10-cm sediment of those experimental cores and then prepared into 1-cm thick slices. For the settling column tests, high initial sediment concentration (West Bay 119.70 kg $m^{-3}$ and Big Mar test with 120.23 kg $m^{-3}$) and low salinity (1 PSU) tests were analyzed for grain size distribution at 3$^{rd}$ hour after the introduction. Samples were collected at each port.

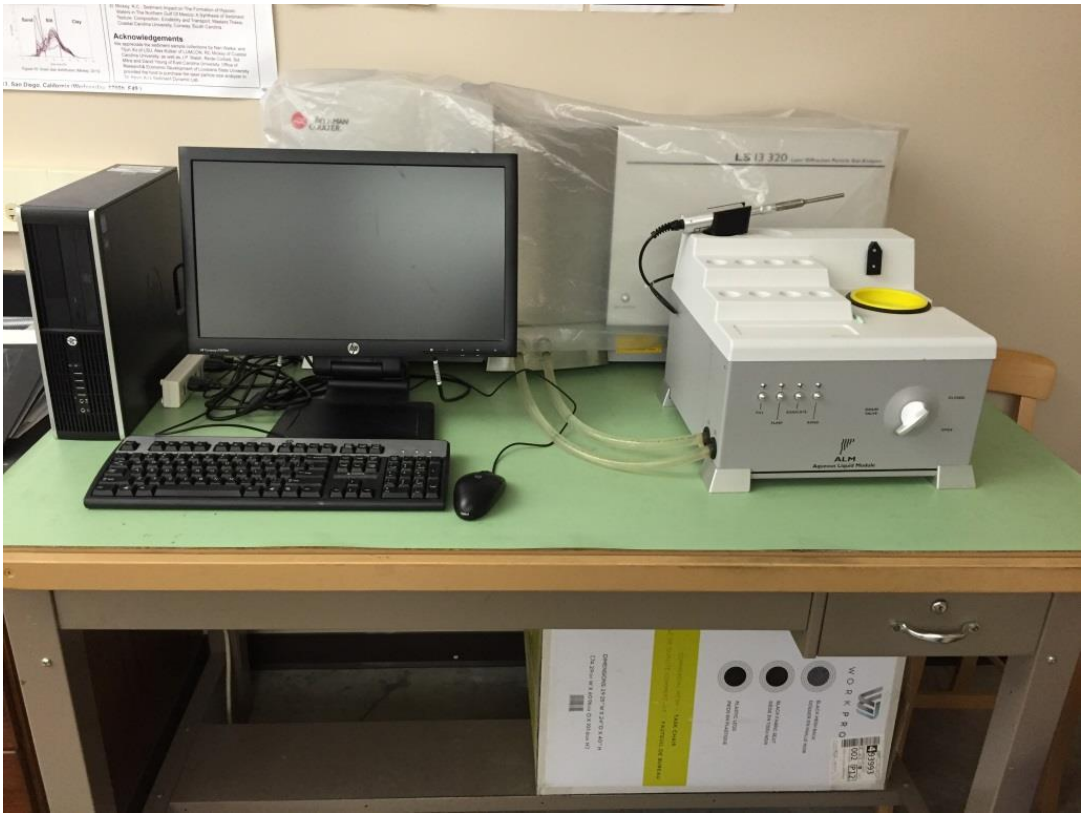


Figure 11. The Beckman-Coulter laser diffraction particle analyzer (Model LS 13 320) used to measure particle size distributions by measuring the light intensity variations of laser beam scattered by particles.

About 1 g of sediment sample was put into a beaker with deionized water to soak for 24 hours. Then the sample was transferred into centrifuge tubes, and 20-30 mL of 30% hydrogen peroxide was added to each tube. Tubes were then water bathed in beakers and left on a hot plate set to 70°C for more than 12 hours to remove any organic matter. After that, the samples were rinsed with deionized water to remove the suspended organic leftovers and put into a centrifuge to separate sediment from water. Samples were disaggregated using a Vortex mixer before placed into the analyzer. When the sample was loaded to the analyzer, sonication was turned on to ensure complete disaggregation. The equation from Folk (1966) was used to convert grain size in mm to the logarithmic unit $\phi$:

$$\phi = -\log_2 d \qquad (3)$$

Then the fractions of sand (>63 μm; $\phi$<4), silt (4–63 μm; $\phi$ is 4–8) and clay (<4 μm; $\phi$>8) were determined.

**2.8 Organic Matter Analysis**

Organic matter amount of push cores WB5 and BM5 (stored in cold room at 4 °C) and untouched experimental cores (stored in room temperature at 21 °C) were measured by the loss-on-ignition method (Heiri et al., 2001). The samples were dried in oven for 48 hours before ground to fine powder using a mortar and a pestle. The fine powder samples were put into dried and pre-weighted crucibles and then combusted in a muffle furnace (Figure 12) at 550°C for about 4 hours. After that, the samples were cool down to room temperature and weighted to calculate the organic content.

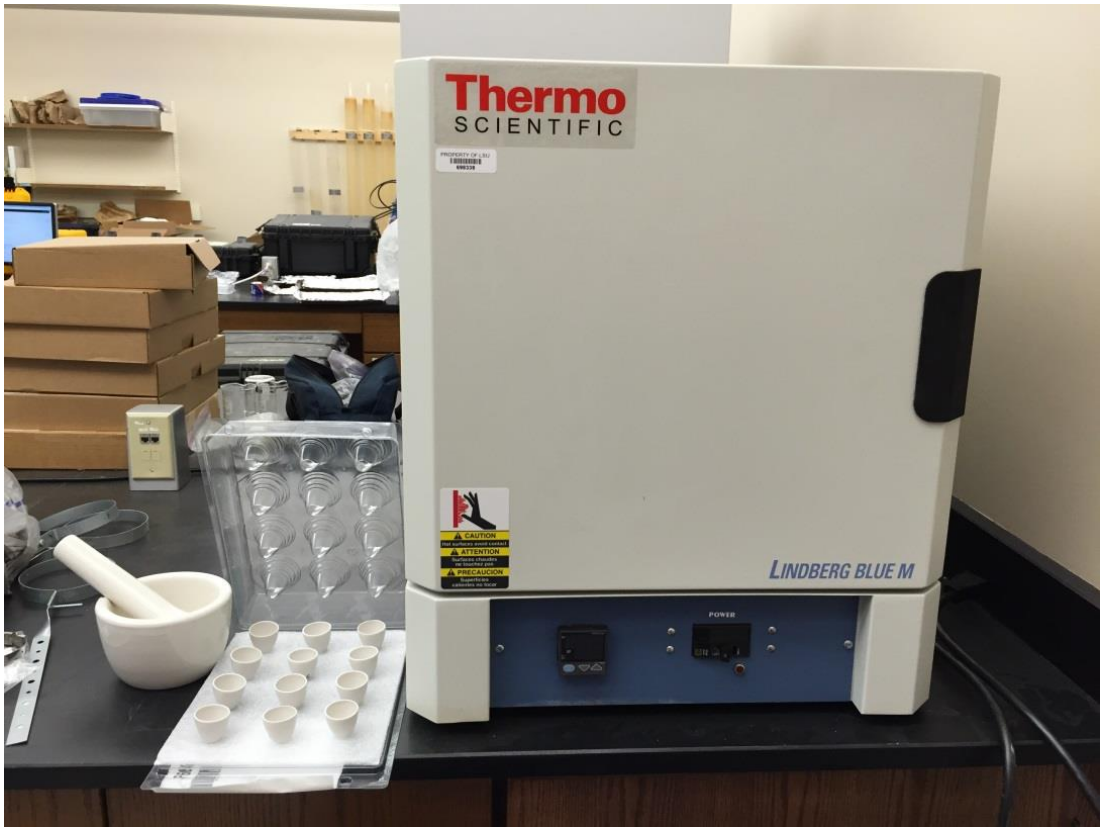


Figure 12. Pestle, mortar, crucibles and muffle furnace used to measure organic matter content using the loss-on-ignition method.

# CHAPTER 3. RESULTS

## 3.1 Erodibility

Two initial sediment concentrations of 62.82 and 123.95 kg $m^{-3}$ were used for West Bay time-series erodibility measurements. The sequence of seven applied shear stresses and duration are shown in Figure 13A, followed by seven time-series turbidities derived from the sediment resuspension in Figures 13B-E. Turbidity curves of both concentrations of West Bay experiments share similar magnitudes and response patterns, except that the half-month result of West Bay at123.95 kg $m^{-3}$ in Figure 14B showed a higher spike around 300 nephelometric turbidity units (NTU) and an early spike under shear stress of 0.1 Pa. The overall trend showed a decreasing turbidity with time (Figures 13-14). For the West Bay 62.82 kg $m^{-3}$ tests, eroded mass were low during the first three stages. No significant turbidity peak was found until a shear stress of 0.2 Pa was applied. The critical shear stress, which is the shear stress that triggered the first significant turbidity spike, shifted from 0.2 Pa (Figure 13B) to 0.45 Pa (Figure 13D). Turbidity of the sediment cores that have been sitting in the laboratory for 5 and 6-month after initial settling did not show obvious peaks during the entire measuring time. The turbidity of Big Mar reached 500 NTU but was only about 200 NTU for West Bay.

The critical shear stress was 0.1 Pa for most Big Mar tests, lower than West Bay's 0.2 Pa results. For the Big Mar 60.11 kg $m^{-3}$ tests, sediment core tested after 2-month of consolidation showed similar turbidity patterns as the core tested after 3 months, so do 4-month and 5-month tests. The core measured after 6-month of consolidations appeared to have strengthened than sediments tested at 2 to 5 months. The Big Mar 120.03 kg $m^{-3}$ tests showed weak correlation between turbidities versus time of consolidation and turbidities were decreased in the first two stages.

Cumulative eroded masses vs. all seven shear stresses relationships were established for all GEMS measurements (Figure 17). Critical shear stresses can also be determined in this figure. Critical shear stress was defined here as the shear stress that generates the first major turbidity spike in the turbidity response figures. In Figures 18A and B, most curves were flat before the 0.2 Pa of shear stress was applied except half month curves, while for Big Mar curves (Figure 17C and D), 0.1 Pa seems to be the breaking point from gentle to relatively steep slopes. In order to demonstrate the exact eroded masses more clearly, cumulative eroded masses at 0.45 Pa of shear stress were extracted and plotted against time of consolidation in Figure 19. In general, West Bay tests showed clear decreasing patterns of the cumulative eroded masses with consolidation time (Figures 18A and B). Tests started with low initial sediment concentrations (60 kg $m^{-3}$, Figure 18A) appeared to have relatively higher cumulative eroded mass than tests started with high initial sediment concentrations (120 kg $m^{-3}$, Figure 18B). $R^2$ of West Bay 62.82 kg $m^{-3}$ and 123.95 kg $m^{-3}$ best fit curves were 0.88 and 0.74, respectively. A decreasing trend was found between 2-month to 4-month tests of Big Mar 60.11 kg $m^{-3}$. Weak correlation between eroded mass and time of consolidation in Big Mar 120.03 kg $m^{-3}$ tests was found in Figure 18D. Organic mats grew on some of the Big Mar sediment surfaces (Figure 19), but based visual inspection during the experiment the mats were all eroded off the core tops before the highest shear stress was applied.

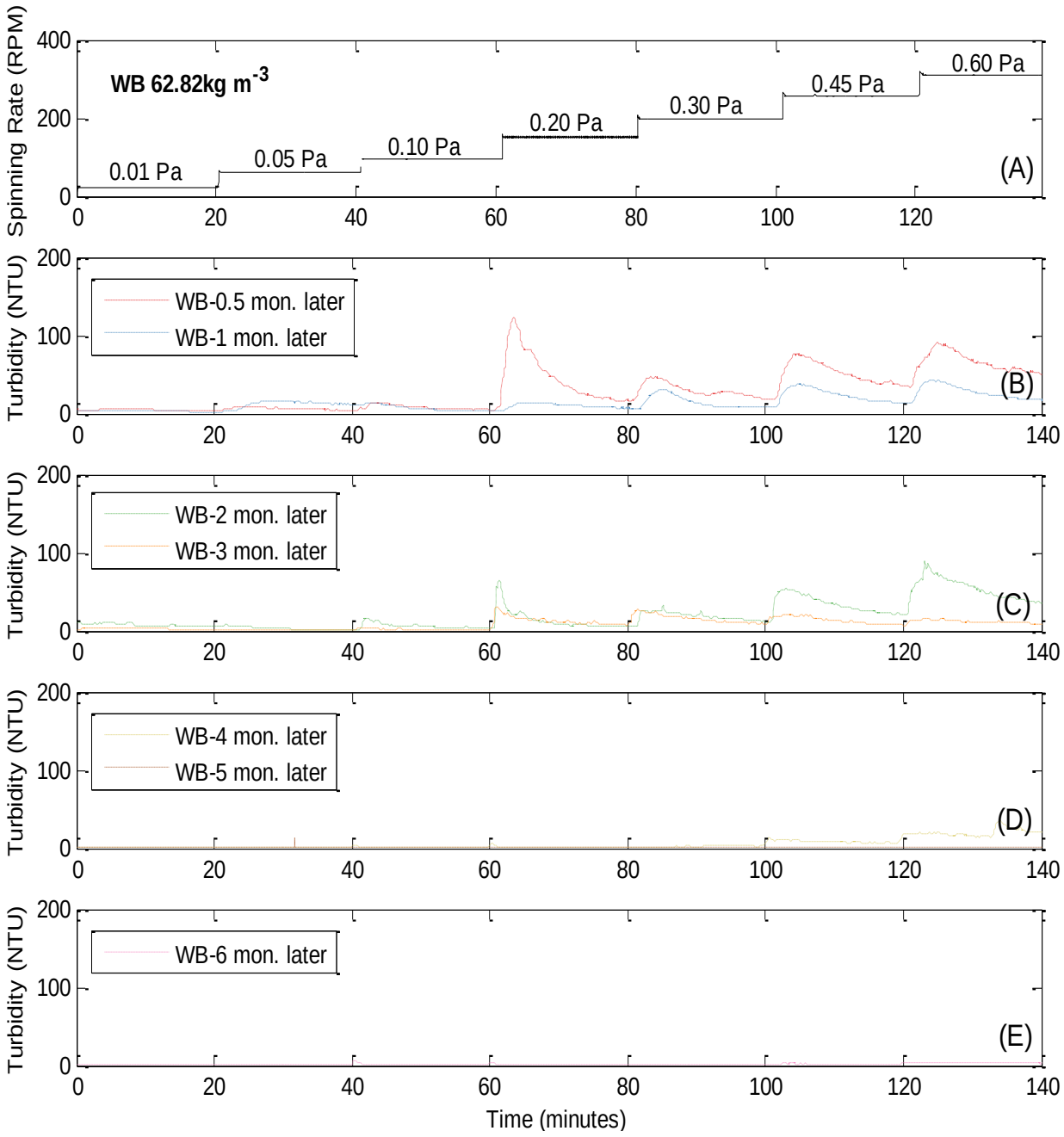


Figure 13. (A) Spinning rate of erosional head (RPM, revolution per minute) and (B–E) turbidity (NTU, nephelometric turbidity unit) of sediment suspended from West Bay experimental core tops with initial sediment concentration of 62.82 kg $m^{-3}$. The seven cores have been sitting in the laboratory for 0.5-6 months respectively and were measured using the dual-core Gust Erosion Microcosm System. Critical shear stress shifted from 0.2 Pa in panel (B) to 0.45 Pa in panel (D).

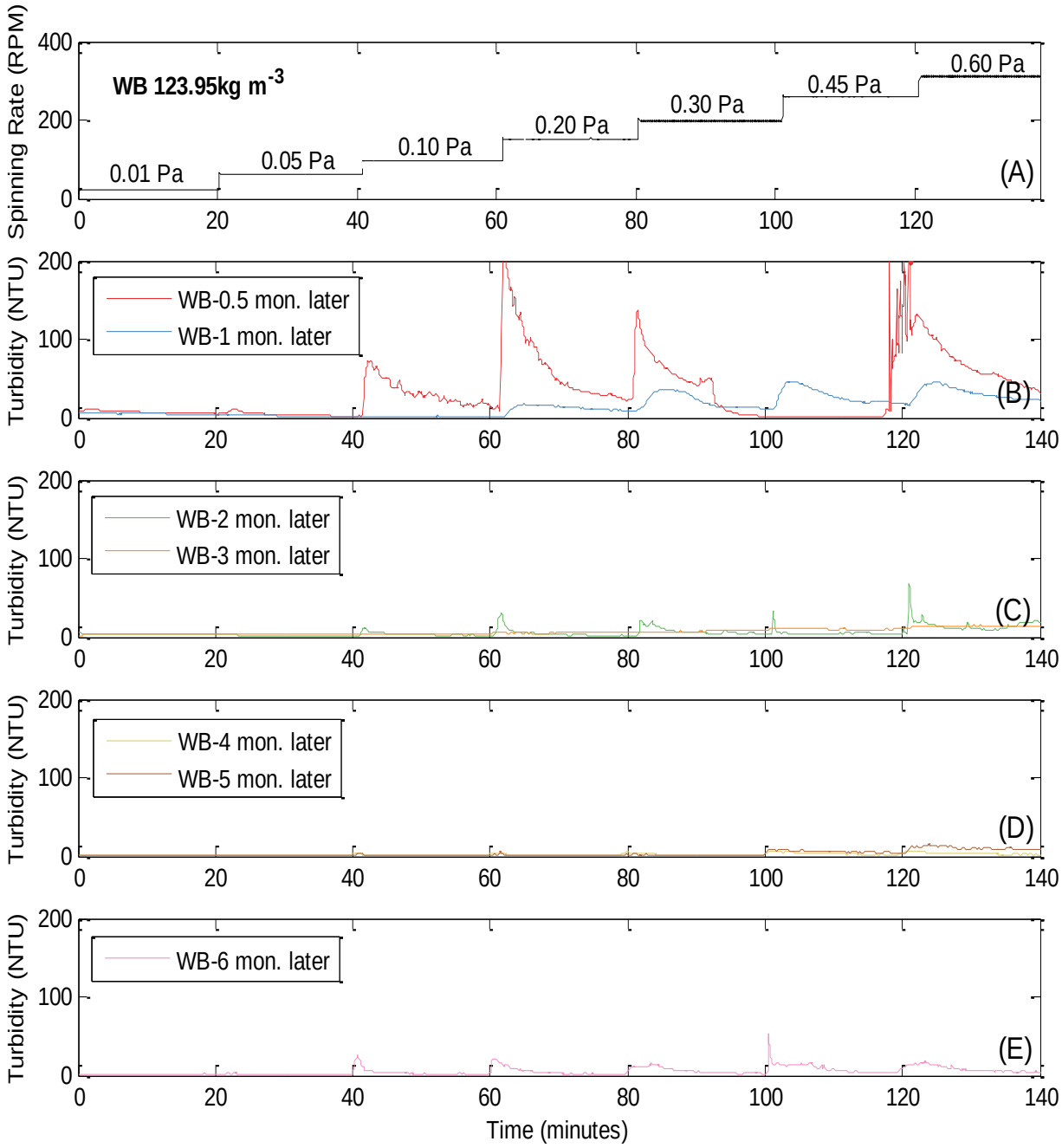


Figure 14. (A) Spinning rate of erosional head (RPM, revolution per minute) and (B–E) turbidity (NTU, nephelometric turbidity unit) of sediment suspended from West Bay experimental core tops with initial sediment concentration of 123.95 kg $m^{-3}$. The seven cores have been sitting in the lab for 0.5-6 months respectively and were measured using the dual-core Gust Erosion Microcosm System.

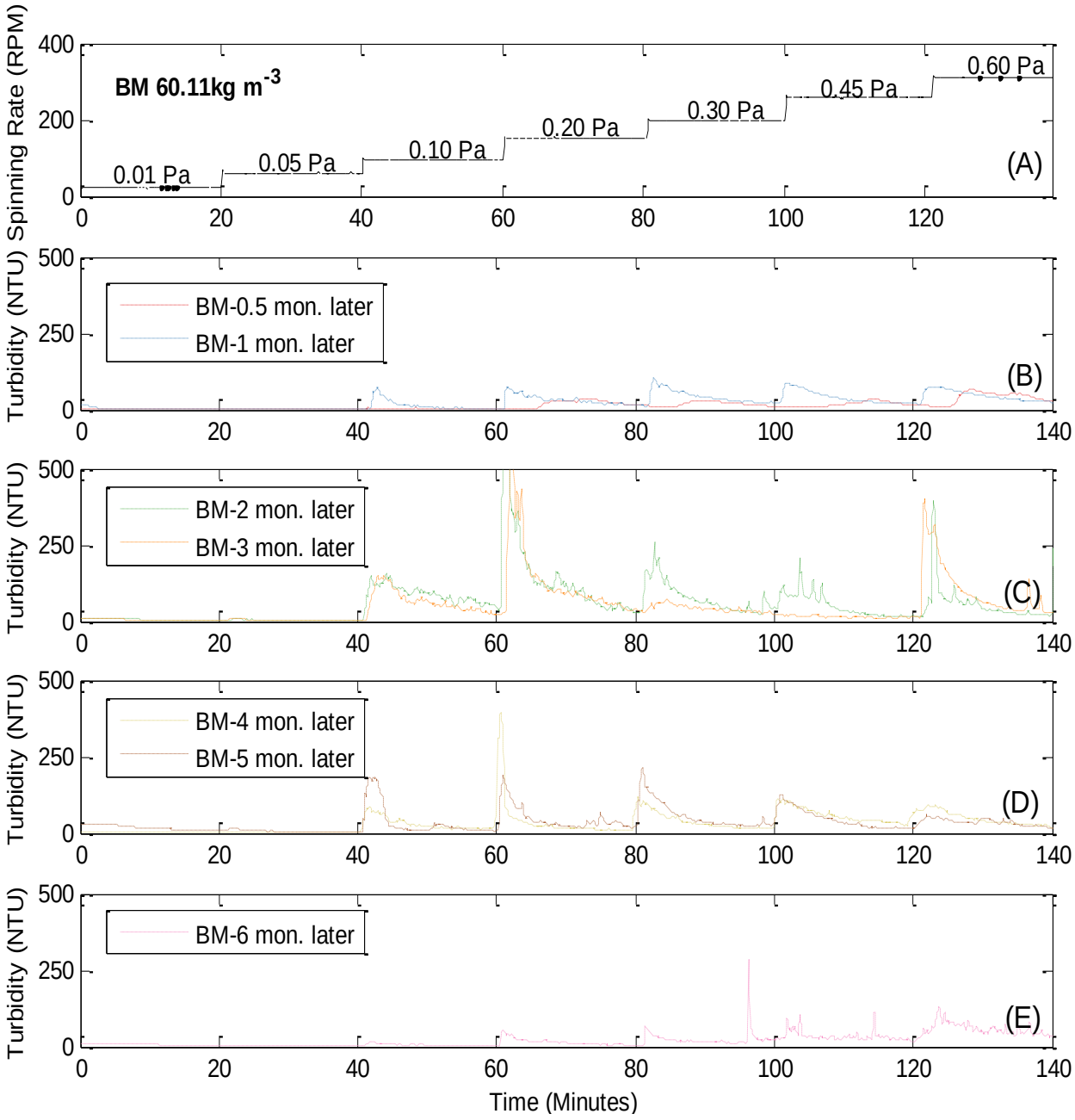


Figure 15. (A) Spinning rate of erosional head (RPM, revolution per minute) and (B–E) turbidity (NTU, nephelometric turbidity unit) of sediment suspended from West Bay experimental core tops with initial sediment concentration of 60.11 kg $m^{-3}$. The seven cores have been sitting in the lab for 0.5-6 months respectively and were measured using the dual-core Gust Erosion Microcosm System.

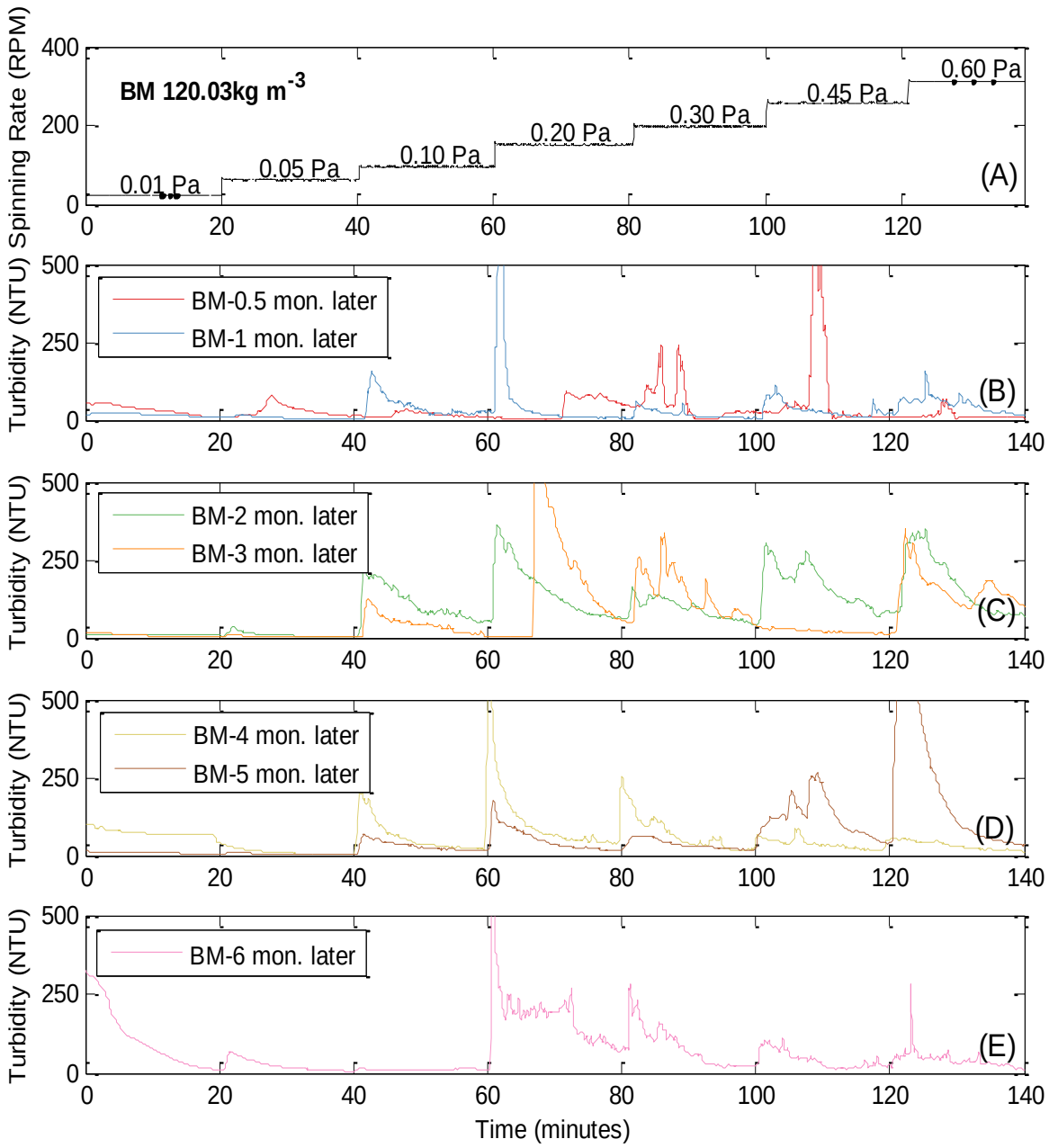


Figure 16. (A) Spinning rate of erosional head (RPM, revolution per minute) and (B–E) turbidity (NTU, nephelometric turbidity unit) of sediment suspended from Big Mar experimental core tops with initial sediment concentration of 120.03 kg $m^{-3}$. The seven cores have been sitting in the lab for 0.5-6 months respectively and were measured using the dual-core Gust Erosion Microcosm System. For the o.5 month test in panel (B), water level was low during the first stage, which was under the 0.01 Pa of shear stress. The water refilling process extended the first stage to 25 minutes before shifted to 0.05 Pa. Hereafter, the turbidity spikes showed about 5 minutes delay.

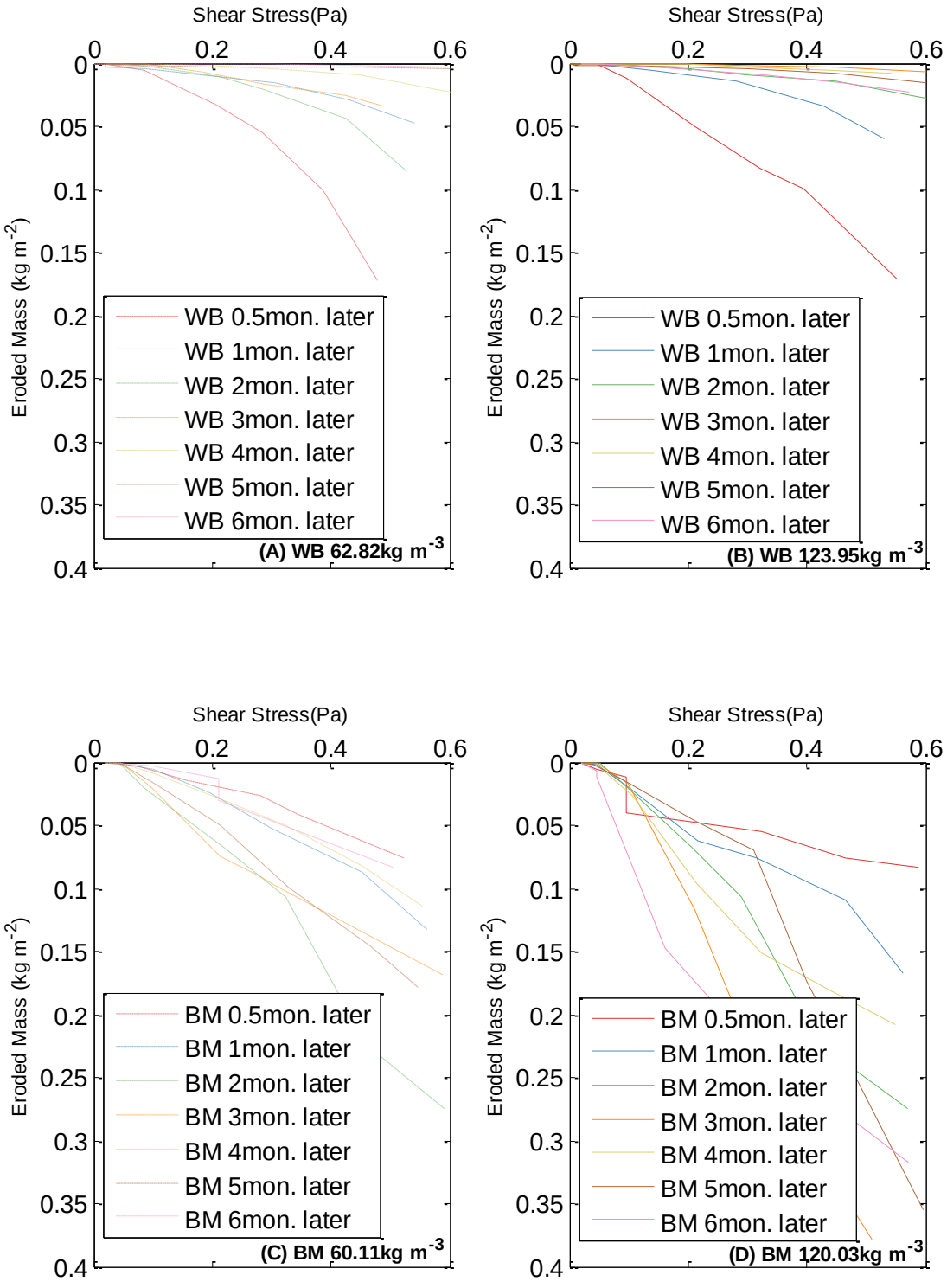


Figure 17. The curves of applied shear stress (Pa) *vs.* eroded mass (kg $m^{-2}$) of total 28 tests for West Bay (A-B) and Big Mar (C-D); dashed lines in (A) and (C) and solid lines in (B) and (D) are experiments started with low initial sediment concentrations and high concentrations, respectively.

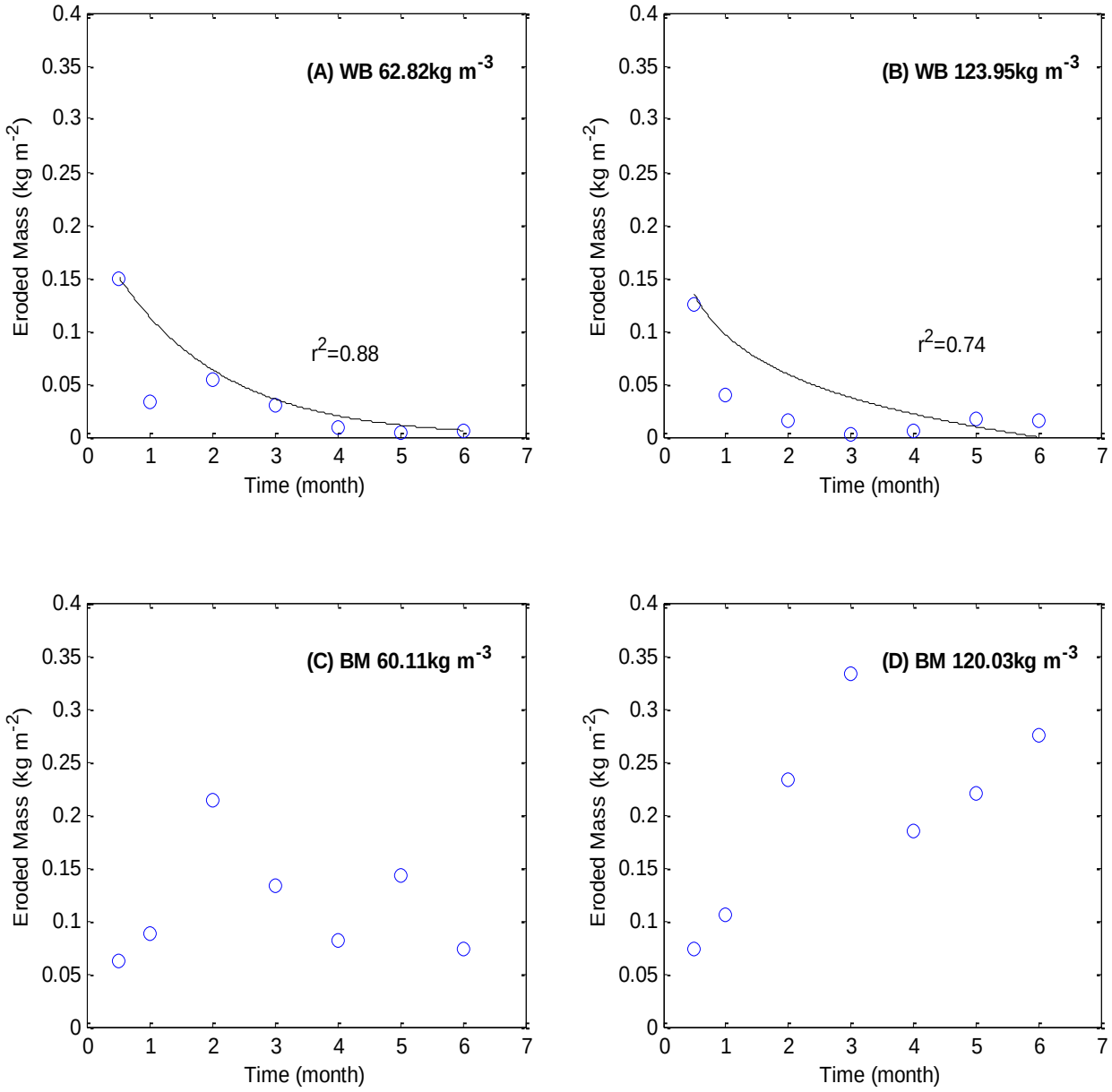


Figure 18. Eroded mass of each core under the shear stress of 0.45 Pa. The black lines in (A-B) are the best fitting curves of for West Bay Gust tests with 62.82 kg $m^{-3}$ ($r^2$=0.88) and 123.95 kg $m^{-3}$ ($r^2$=0.74) initial sediment concentrations, respectively. Big Mar tests showed weak correlations between eroded mass and settling time, which may be related to relative high organic matter when compared to West Bay.

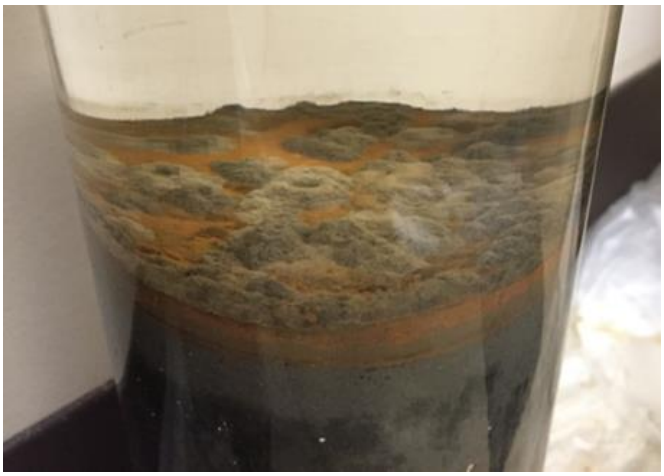

Figure 19. Picture of organic mats growing on GEMS core sediment surface (in room temperature).

### 3.2 Consolidation

Time-series measurements of dry sediment mass concentration at each sampling port during the settling process were conducted for four initial concentrations with two salinities. All initial concentrations belong to the range of hindered settling (Whitehouse et al., 2000a). Sediments settled quickly within the first few hours. The difference between two salinities (1 PSU and 5PSU, Figure 20) was the sharpness of the change in the elevation of water-sediment interface. High salinity (5PSU) tests showed a sharp concentration gradient between clear water (above) and water with suspended sediment (below), or zone settling (Palermo and Thackston, 1988). However, the low salinity (1 PSU) tests appeared to be homogenous within the first few hours. After that, a water-sediment interface was found at the bottom of the column with sediments kept depositing on top of it. Fine sediments were still suspended as flocs in water above the interface, which also gave another strong vertical concentration gradient, also called lutocline (Figure 21) on top (Ross and Mehta, 1991).


Figure 20. Comparison of lutoclines in different salinity tests. Settling column experiment of West Bay 10 kg $m^{-3}$ test with different salinities, (A) 5 PSU, (B) 1 PSU, pics were taken at the $25^{th}$ hour after introduction.

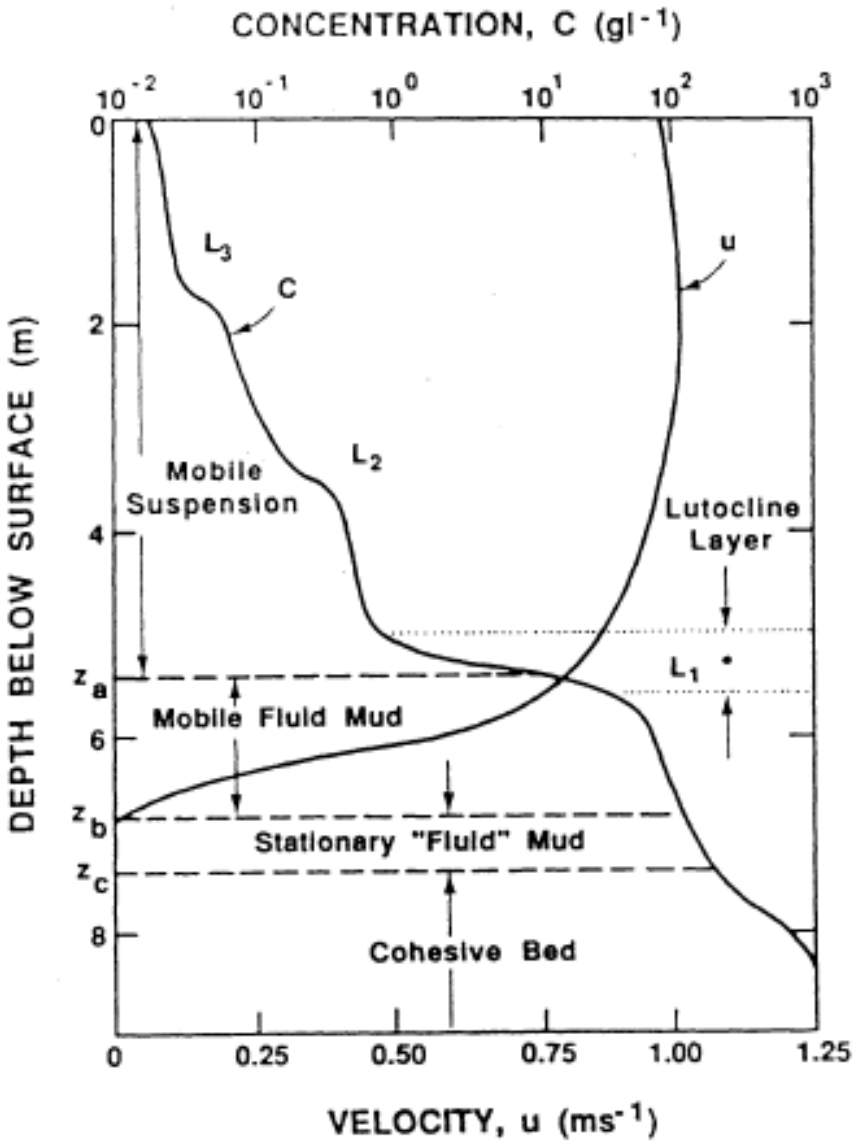


Figure 21. Typical instantaneous concentration and velocity profiles in high concentration estuarine environment (Ross and Mehta, 1989).

Sampled sediment concentrations increased with depth during each sampling period (Figure 22-25). For most tests higher than 10 kg $m^{-3}$ initial concentration, sediment at the lowest port can reach a high dry bulk density value in one hour in low salinity tests, but about three hours in high salinity tests. Within a few hours, concentrations increased quickly at the 10 and 30 cm elevation, but more obvious at the 10 cm elevation between two sampling events (Figure 22-25). Concentration at the lowest sampling port shows that tests started with a higher initial

sediment concentration reached a higher final concentration compared to lower initial concentration tests. For the similar initial concentration tests, low salinity tests shows relatively higher final concentration than high salinity tests.

Normalized sediment surface heights were plotted against sampling time in Figure 26. Test started with the lowest sediment concentration showed the fastest settling in the first several hours and reached the asymptotic height faster than the higher initial concentration test. High salinity tests ended with higher heights than low salinity tests. The height decreasing rate of sediment bed had a negative correlation with the increasing initial sediment concentrations (Figures 22-25). The Big Mar time-series normalized height changes were compared with Lo et al. (2014) Lake Lery data in Figure 28. Big Mar showed relatively faster settling and lower final heights when compared with Lo's similar initial sediment concentration tests.

Time for each test at which the sediment surface reached half of its initial height ($t_{50}$) was extracted from the raw dataset and plotted against initial sediment concentration ($C_0$) in a log-linear plot (Figure 28). West Bay and Big Mar tests showed similar $t_{50}$ for high salinity (5 PSU) tests while relatively larger difference in low salinity (1 PSU) tests. It is clear that low salinity tests settled faster than high salinity ones.

Grain size distributions were plotted for low salinity (1 PSU) tests with 120 kg $m^{-3}$ initial sediment concentration in Figures 29 and 30. The results show coarsening downward trend, which matches the common sense of coarse sediment settles faster than finer sediment, except slightly coarser particulates were suspended at the water surface.

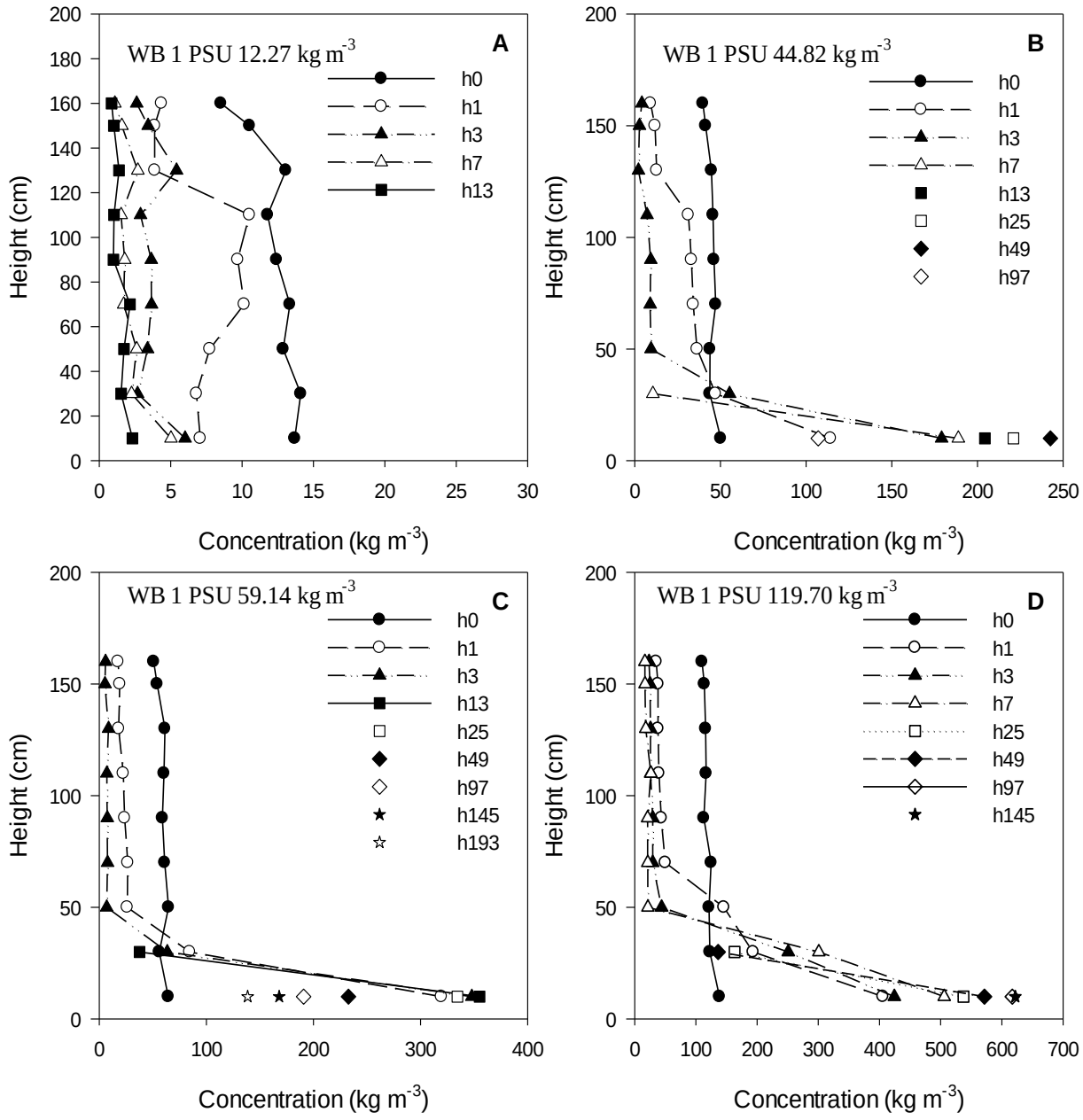


Figure 22. Time series of suspension dry bulk density with 12.27, 44.82, 59.14 and 119.70 kg m$^{-3}$ initial sediment concentrations and a salinity of 1 PSU for West Bay consolidation tests, labeled by sampling time since the beginning of experiments.

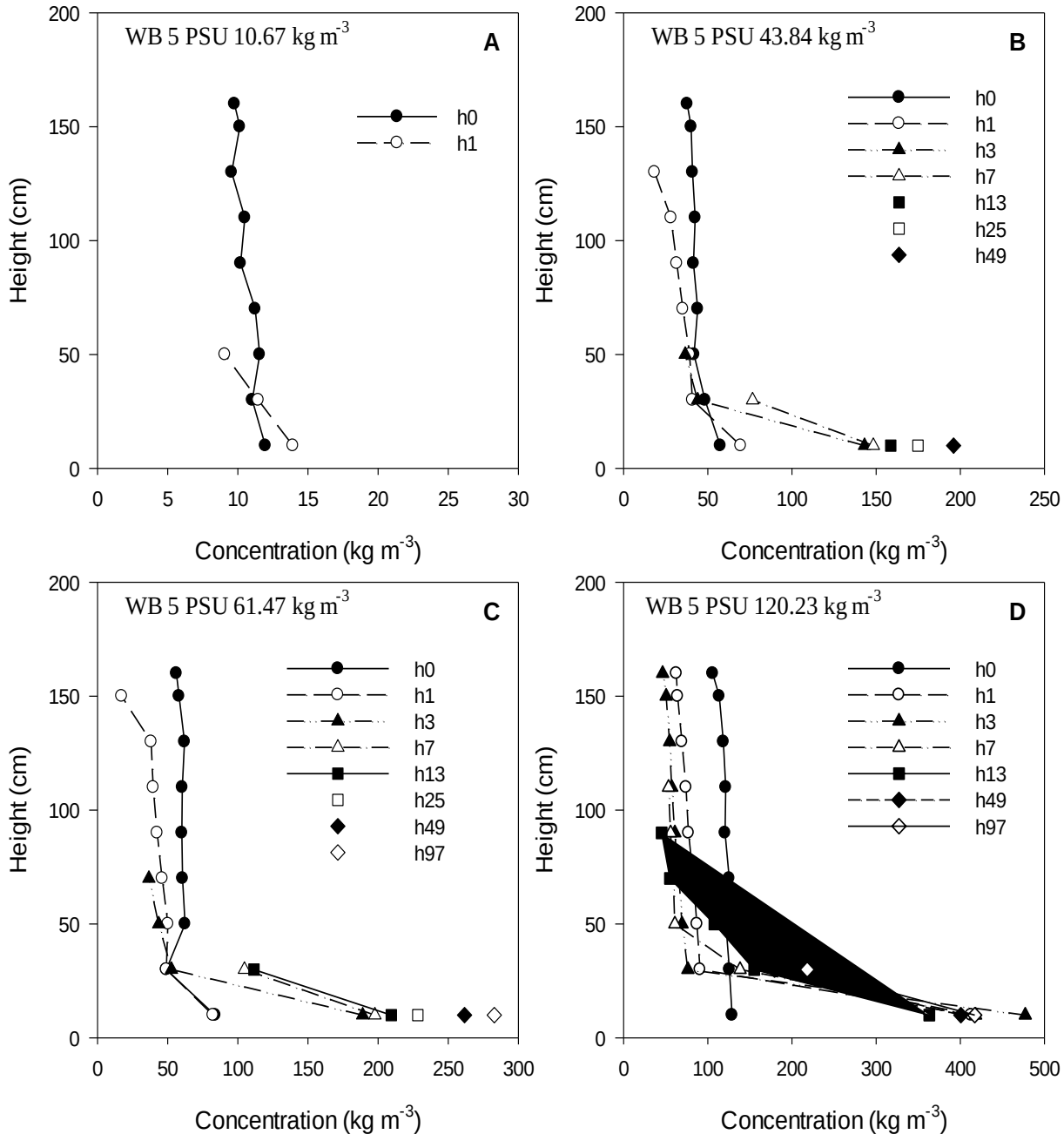


Figure 23. Time series of suspension dry bulk density with 10.67, 43.84, 61.47 and 120.23 kg m$^{-3}$ initial sediment concentrations and a salinity of 5 PSU for West Bay consolidation tests, labeled by sampling time since the beginning of experiments.

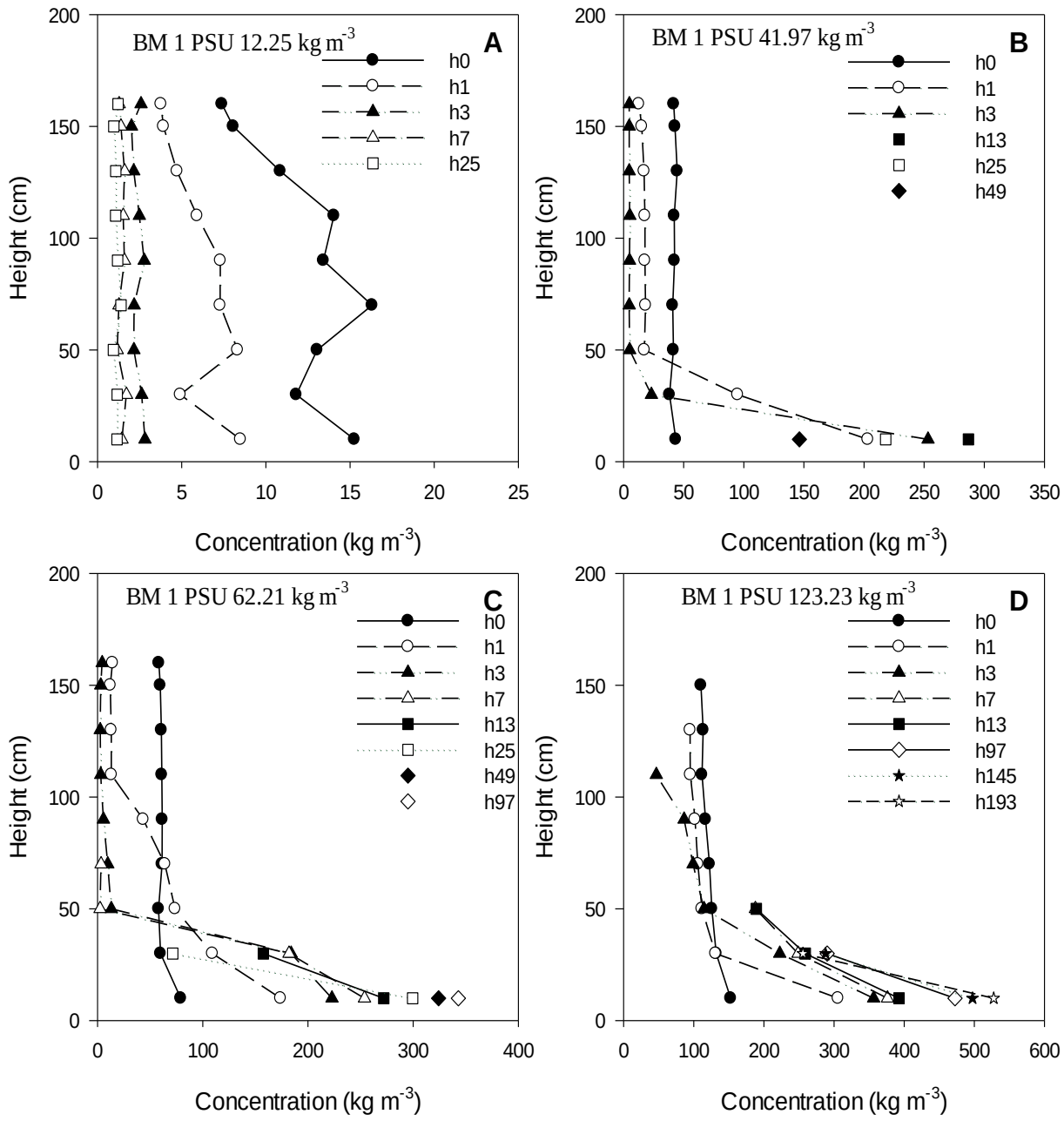


Figure 24. Time series of suspension dry bulk density with 12.25, 41.97, 62.21 and 123.23 kg m$^{-3}$ initial sediment concentrations and a salinity of 1 PSU for Big Mar consolidation tests, labeled by sampling time since the beginning of experiments.

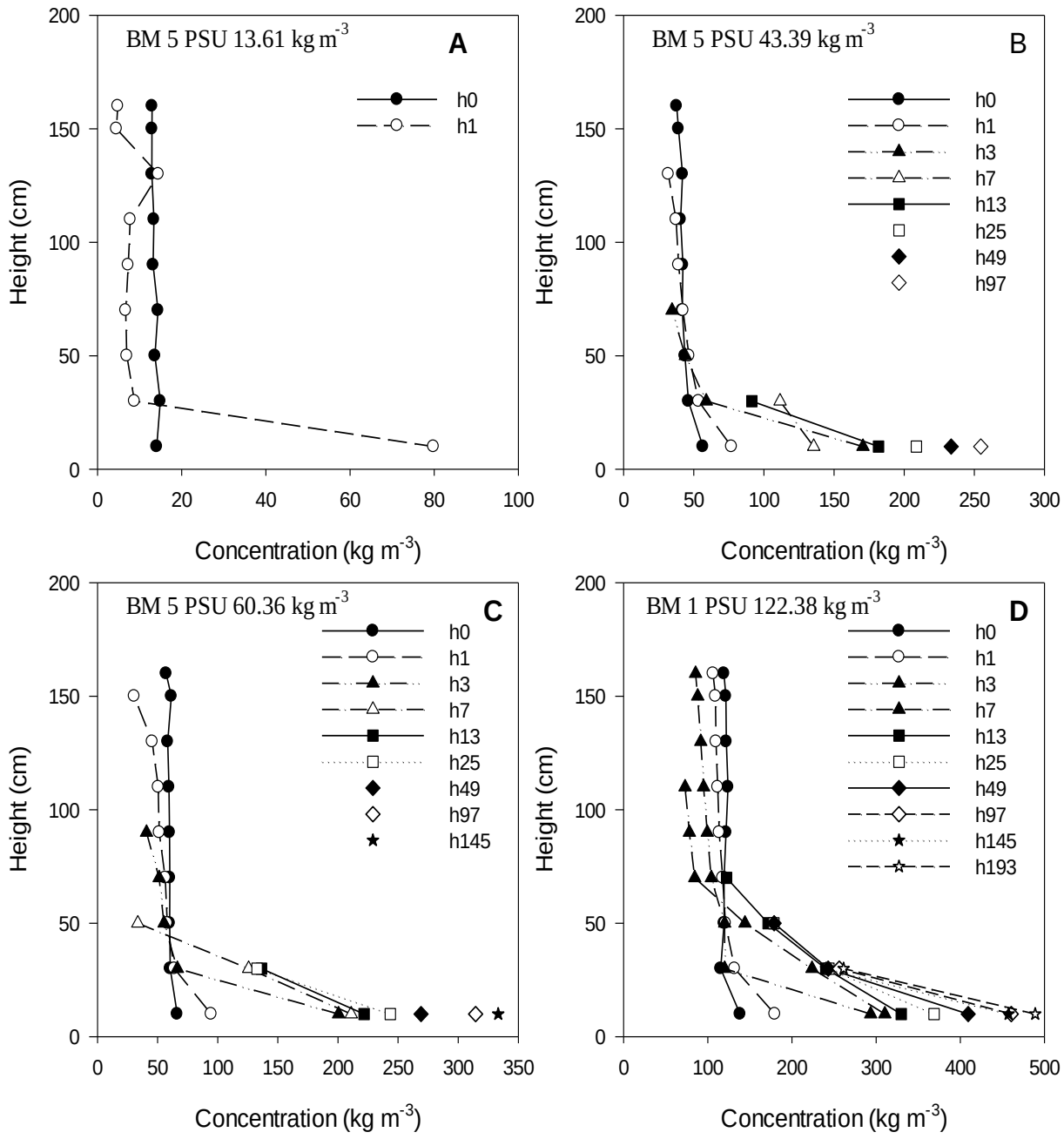


Figure 25. Time series of suspension dry bulk density with 13.61, 43.39, 60.36 and 122.38 kg m$^{-3}$ initial sediment concentrations and a salinity of 5 PSU for Big Mar consolidation tests, labeled by sampling time since the beginning of experiments.

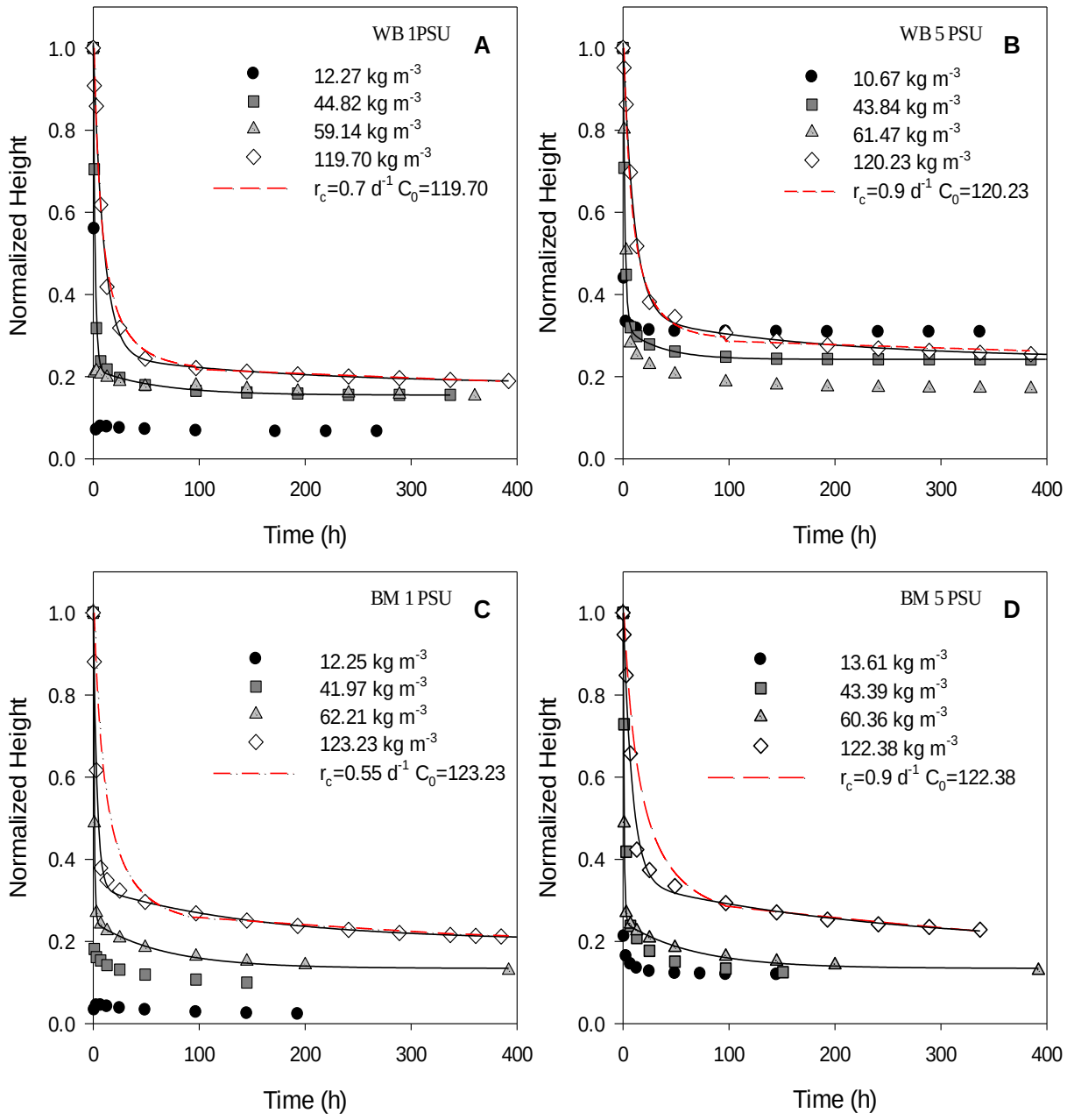


Figure 26. Composite plot of normalized sediment suspension height vs. time for each settling column tests, labeled by initial sediment concentrations. Black lines are regression results with $r^2$=0.99. Sanford (2008) model results were plotted as red curves with a consolidation rate of 0.9 $d^{-1}$ for different initial sediment concentrations with defined initial and boundary conditions.

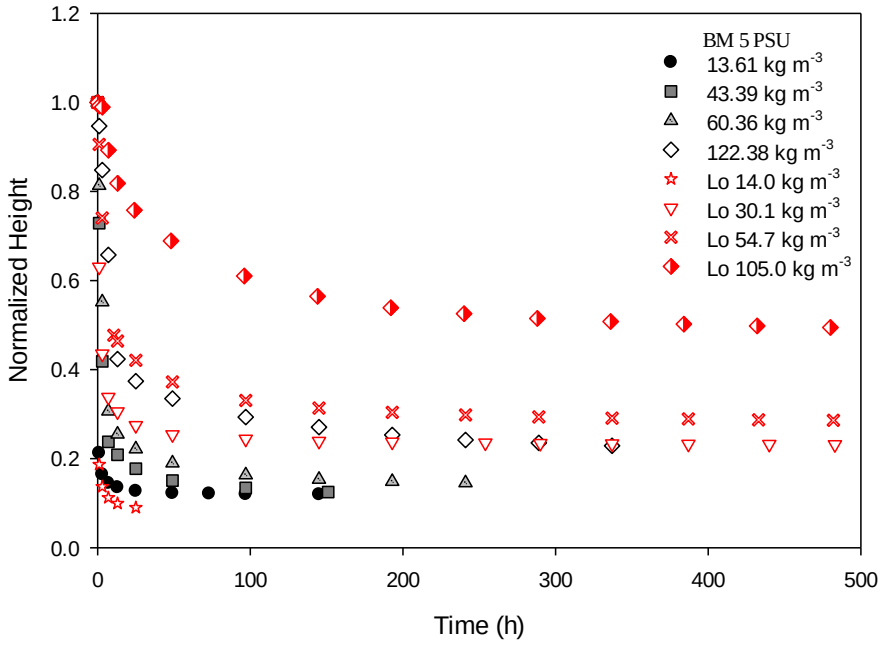


Figure 27. Big Mar 5 PSU time-series normalized sediment bed height compared with Lo (2014) Lake Lery 5 PSU results, labeled by initial sediment concentrations.

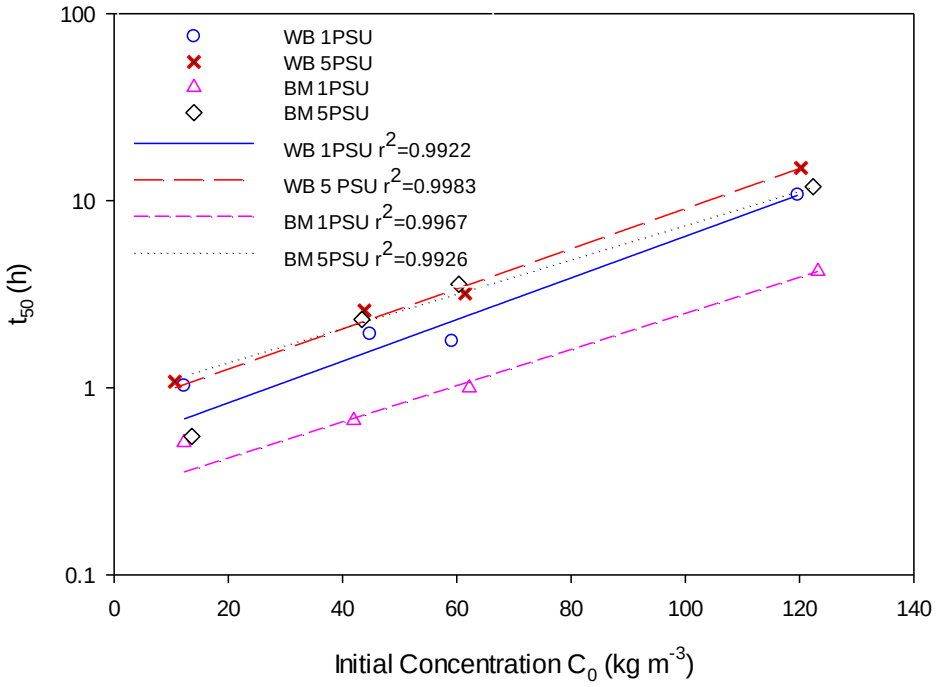


Figure 28. Regression analysis of $t_{50}$ (time for the sediment suspension to reach half of its initial height) vs. initial sediment concentration, labeled by salinities. The lines are regression results for $C_0$ and $t_{50}$ with good fitness.

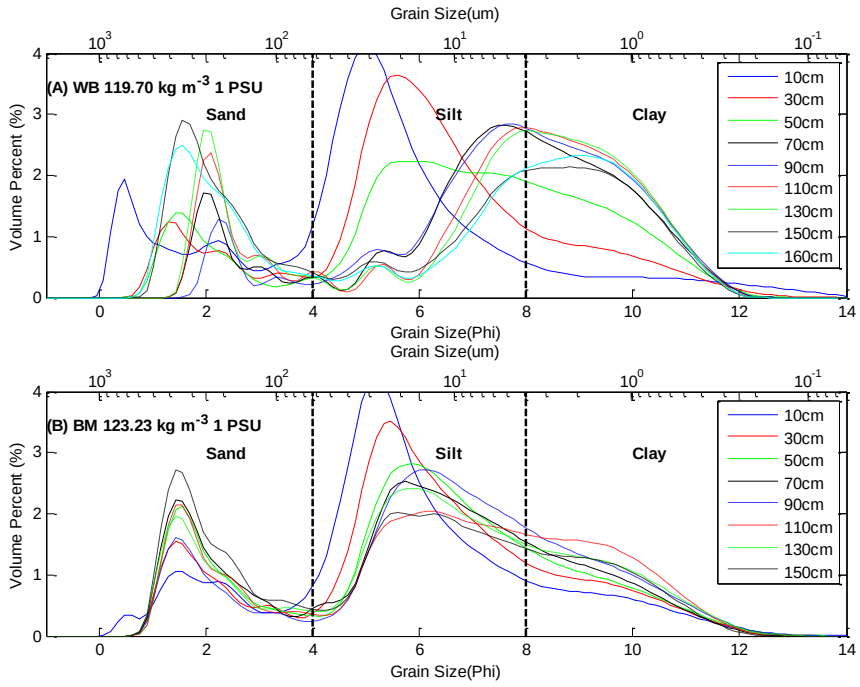


Figure 29. West Bay (A) and Big Mar (B) grain size distributions for low salinity (1 PSU), high initial sediment concentration (120 kg m $^{-3}$) tests in the settling column after 3 hours of settling. 10-150cm are the heights above the base of settling column.

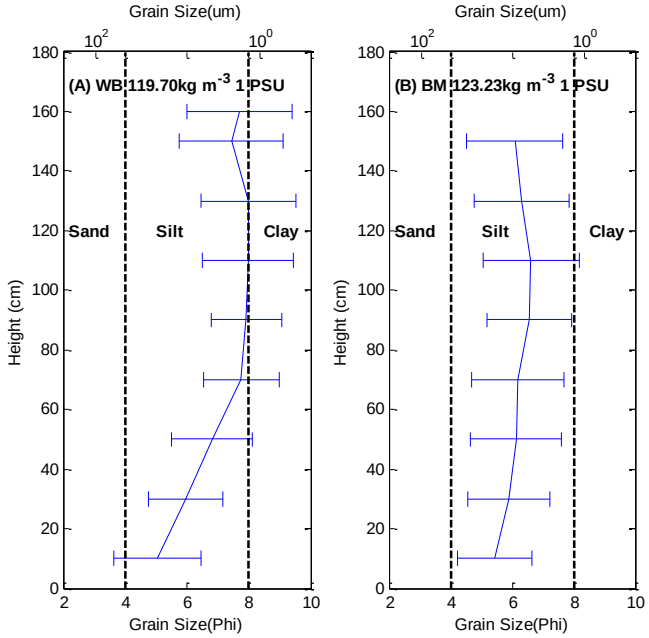


Figure 30. West Bay (A) and Big Mar (B) median grain size spatial distributions for low salinity (1 PSU), high initial sediment concentration (120 kg m $^{-3}$) tests in the settling column after 3 hours of settling. Bars are standard deviations of grain size distributions.

### 3.3 Grain Size

Down-core grain size data of pushcores WB5 and BM5 indicated that silt is the most abundant grain size in both study sites (Figure 31). West Bay has a higher content of sand than that of Big Mar. The length of push core WB5 was 85 cm and that of BM5 was 70 cm.

Figures 32 and 33 show the surficial grain size distributions of top 10 cm of West Bay and Big Mar experimental cores that were prepared in 200-cm and 50-cm tubes and have been sitting in the laboratory for twelve and seven months, respectively. Typical bimodal pattern was found in all the figures. Mean grain sizes were extracted and plotted against the depths to show the spatial grain size distribution (Figure 34). The mean grain size did not varied much due to the small scale of the depth and it was concentrated in the silt range. The overall trends were fining upward in all cores. This trend can be seen more clearly in the grain size mode distribution plots (Figure 35).

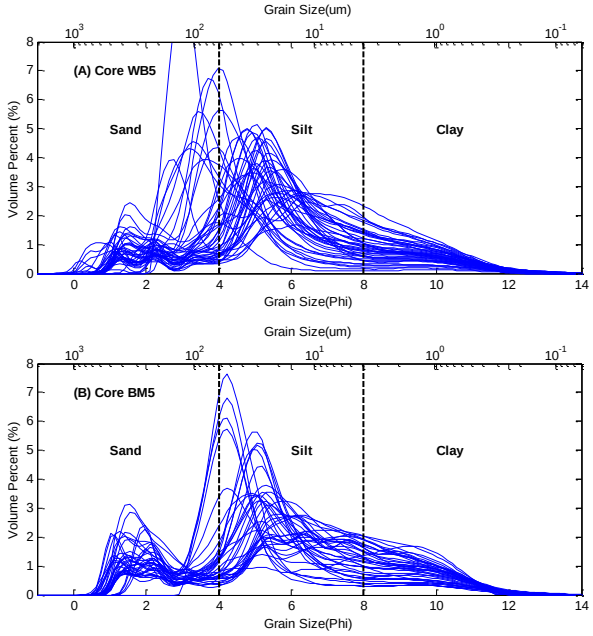


Figure 31. Grain size distributions of down-core sediment of push core WB5 in West Bay (A) with a total length of 85 cm, and push core BM5 in Big Mar (B) with a total length of 70 cm (Xu et al., 2016).

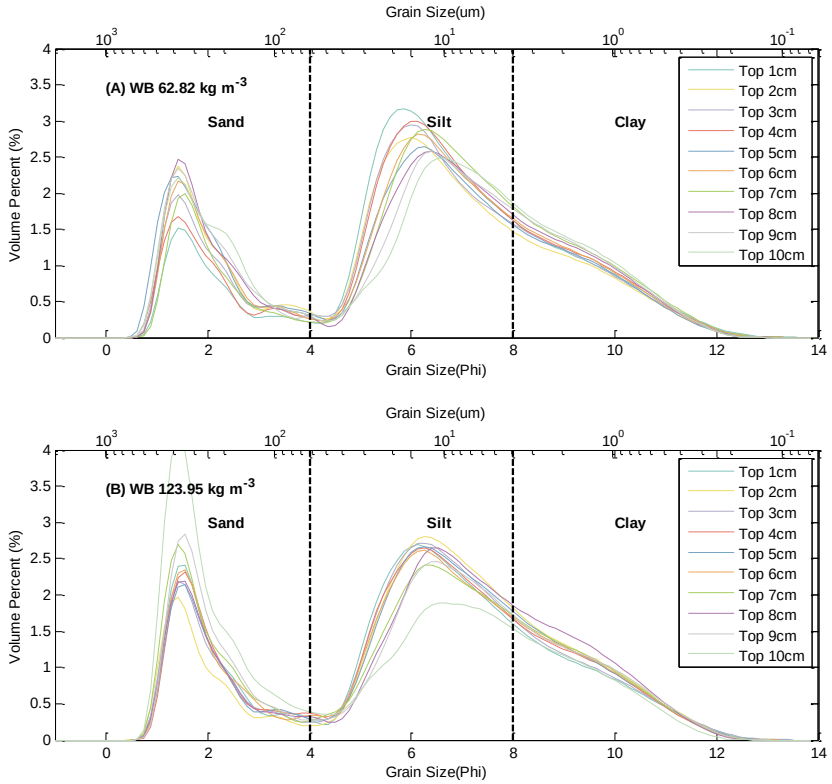


Figure 32. Grain size distributions of top 10 cm of West Bay experimental cores formed after settling for twelve months in the laboratory.

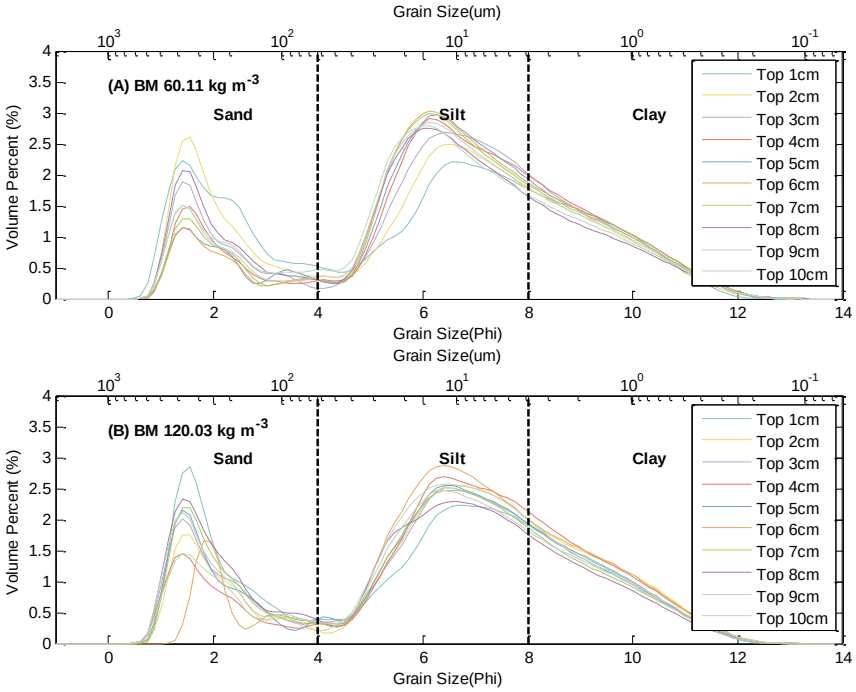


Figure 33. Grain size distributions of top 10 cm of Big Mar experimental cores formed after settling for seven months in the laboratory.

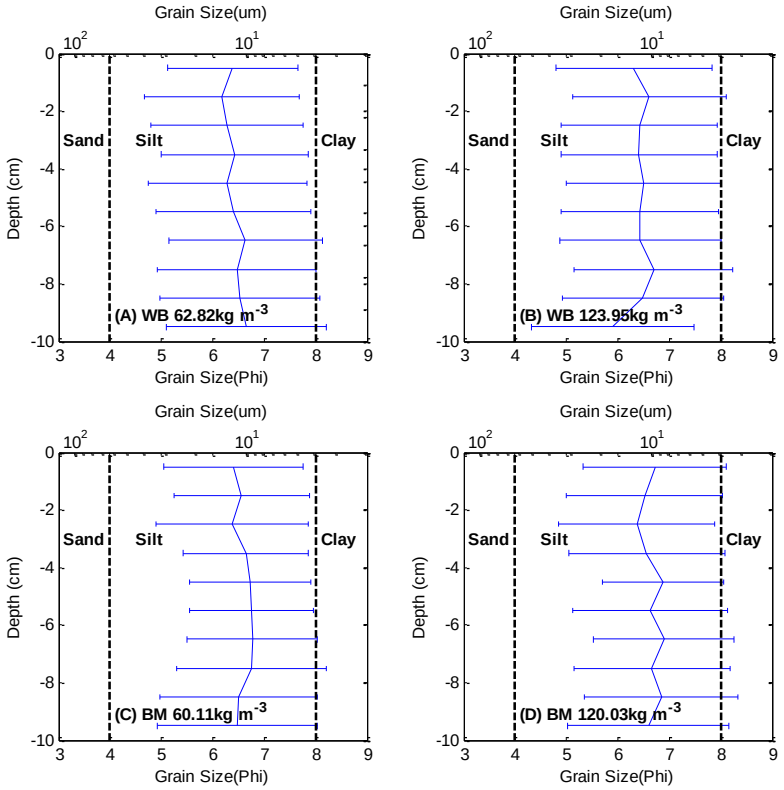


Figure 34. Median grain size distributions of top 10 cm of West Bay and Big Mar experimental cores formed after twelve months and seven months of settling in the laboratory, respectively. Error bars indicate standard deviations.

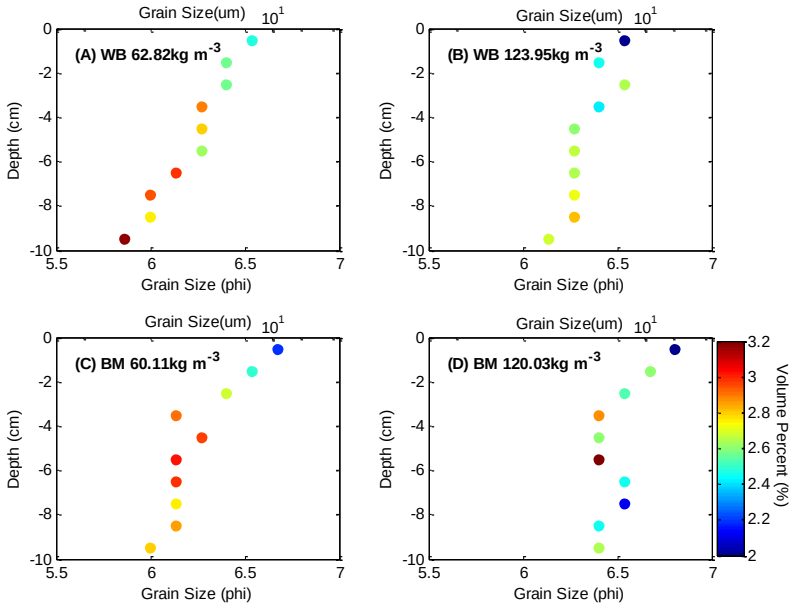


Figure 35. Color volume-frequency plots of grain size modes (tallest peaks) distributions of top 10 cm of West Bay and Big Mar experimental cores formed after twelve months and seven months of consolidation in the laboratory, respectively.

### 3.4 Organic Matter

Organic content of both experimental cores (Figure 36) prepared in the laboratory and push cores (Figure 37) collected in the field was plotted against the depths. Although the experimental cores have been sitting in the laboratory under room temperature for more than a half year, there were still some organic matter remained in the cores, decreasing from the core surface to depth. The overall value and trend were similar in West Bay and Big Mar experimental cores but the averaged organic content of Big Mar original core was 10.57%, almost twice as much as West Bay which was 5.56% (Table 2). Organic matter appeared to settle slower than most of the sediments due to its relatively lower density. Once all sediments have settled and started to consolidate, some organic mats developed on top of some Big Mar GEMS core surfaces. Cores with little to no organic mats were selected to be used in the GEMS measurements. For cores with small organic mats, all mats were eroded off the sediment surfaces before the highest shear stress was applied during the erodibility measurements.

Table 2. Averaged organic matter percent of surficial sediment in both experimental and original sediment cores of West Bay and Big Mar.

| Study Area | Cores | Depth(cm) | Averaged Organic Matter Percent of Surficial Sediment (%) |
|---|---|---|---|
| West Bay | Initial concentration at 62.82 kg $m^{-3}$ | Top 10 | 7.74 |
| | Initial concentration at 123.95 kg $m^{-3}$ | Top 10 | 8.42 |
| | Pushcore WB5 | Top 20 | 5.56 |
| Big Mar | Initial concentration at 60.11 kg $m^{-3}$ | Top 10 | 9.28 |
| | Initial concentration at 120.03 kg $m^{-3}$ | Top 10 | 8.85 |
| | Pushcore BM5 | Top 20 | 10.57 |

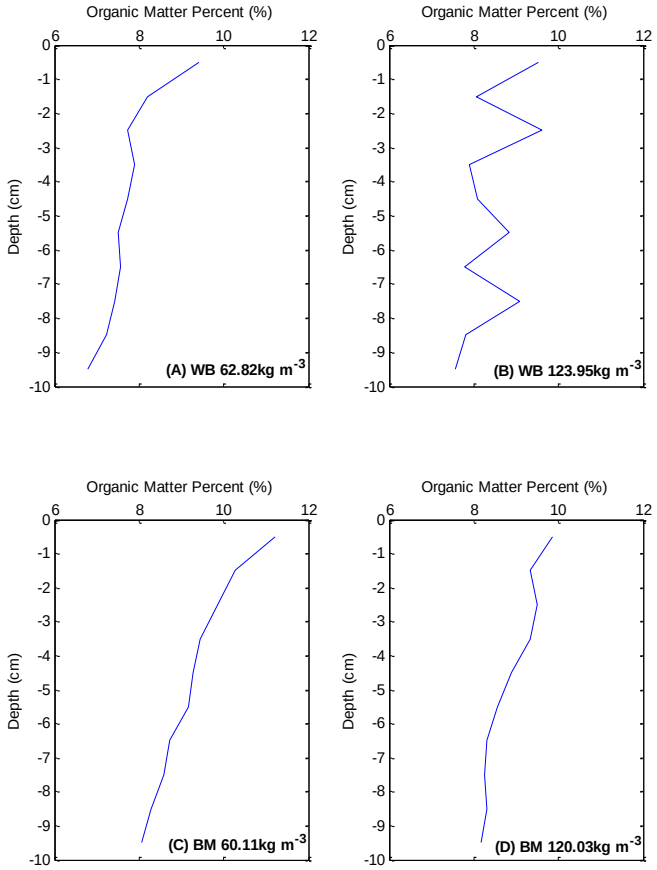


Figure 36. Organic matter percent of top 10 cm of experimental cores formed after settling in the laboratory. (A-B) are results of West Bay cores which have been sitting in the laboratory for twelve months. (C-D) are results of Big Mar cores which have been sitting in the laboratory for seven months.

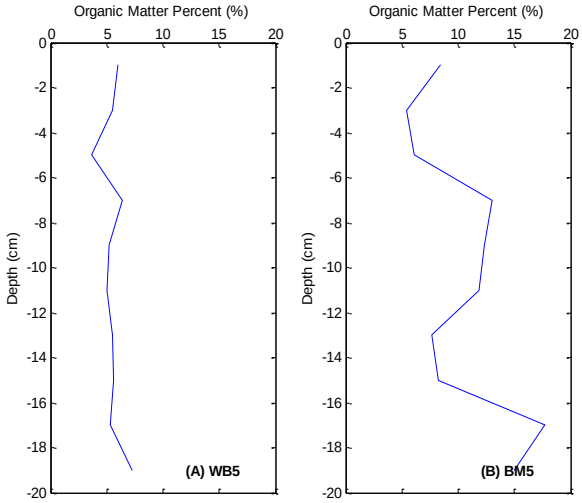


Figure 37. Top 20 cm surficial organic matter percent of push cores WB5 from West Bay (A) and BM5 from Big Mar (B).

# CHAPTER 4. DISCUSSION

## 4.1 Erodibility

### 4.1.1 Influencing factors

Sediment erosion occurs when waves/currents induced shear stress ($\tau_b$) exceeds the critical shear stress ($\tau_c$) which can be considered as the shear stress that triggers the first major turbidity peak in GEMS measurements. Unlike non-cohesive sediments in which $\tau_c$ is mainly dependent on grain size, cohesive sediment erodibility is related to salinity, flocculation, consolidation, particle size distribution, biological effects and many others (Black, 1997; Parchure and Mehta, 1985; Roberts et al., 1998; Wiberg and Smith, 1987).

### 4.1.2 Critical shear stress and turbidity

The critical shear stress of West Bay experimental cores (Figures 14, 15 and 18) was 0.2 Pa for 0.5 1, 2 and 3-month tests and moved up to 0.45 Pa for 4-month test. The value of 0.2 Pa matches the field erodibility measurement result (Xu et al., 2016). The critical shear stress of Big Mar experimental cores was around 0.1 Pa for 0.5-5-month tests (Figures 15, 16 and 17), which was lower than the field results of 0.2 Pa (Xu et al., 2016). The critical shear stress increased from 0.1 Pa to 0.2 Pa in 6-month test. The observed increase in critical shear stresses was an evidence of sediment consolidation with time.

The overall turbidity values of West Bay 62.82 and 123.95 kg $m^{-3}$ measurements are decreasing with increasing time of consolidation (Figures 13-14), but the 123.95 kg $m^{-3}$ cores were more consolidated in 2 and 3-month measurements (Figures 13-14C) than that of the 62.82 kg $m^{-3}$ measurements. Because the critical shear stress is generally positively related to sediment mass concentration, higher shear stress is needed to erode the surficial sediments off the core top for high concentration sediment than for low concentration sediment (Jepsen et al., 1997).

The overall turbidity values of Big Mar 60.11 and 120.03 kg $m^{-3}$ measurements start to show the decreasing trend with increasing time of consolidation since 3-month of consolidation (Figures 16-17). This trend can be seen in 60.11 kg $m^{-3}$ measurements than that of 120.03 kg $m^{-3}$ measurements. Big Mar 60.11 kg $m^{-3}$ measurements show smaller turbidity values than its high sediment concentration measurements. Cores that were formed with higher initial sediment concentrations may contain higher organic matter content in sediment and more organic mats may grow on core tops when compare with that of cores formed with relatively lower initial sediment concentrations. The difference in organic matter content may lead to the different responses to the applied shear stresses between Big Mar high and low sediment concentration measurements (Venier et al., 2012).

The decreasing trend of turbidity values with increasing time of consolidation in Big Mar measurements is not as 'regular' as that of West Bay measurements when comparing measurements with the same sediment concentrations (Figures 13-16). This trend can be found from the first curve (0.5-month) to the last one (6-month) in West Bay measurements (Figures 13-14 B-E). But only can be found in the 3-month curve to the 6-month curve in Big Mar measurements (Figures 15-16 C-E). These differences may also be related to organic matter amount differences in two sediment sources (Table 2). Winterwerp and van Kesteren (2004) pointed out that organic matter can have large effects on the flocs formation and sediment bed stability.

For the West Bay 123.95 kg $m^{-3}$ measurements, the low turbidity response for 0.5-month measurement under the shear stress of 0.45 Pa (Figure 14B) was actually caused by an accidental low water level in the sediment chamber due to a leaking problem in the tubing (between the spinning disk in the erosional head and the core top). The spinning disc couldn't reach the water

surface so there was no shear stress to trigger erosion on the sediment surface during that period and water had to be refilled in the middle of experiments, and similar problem happened during the Big Mar 3-month test of 120.03 kg $m^{-3}$ under 0.45 Pa of shear stress (Figure 16C) and the delayed spikes in half-month and 3-month test under 0.2 Pa of shear stress (Figure 16 B-C) were also caused by water refilling processes. The turbidity spiked around 300 NTU when water was filled up again.

Xu et al. (2016) calculated the wave-induced shear stresses under the influence of fetch of the bay and concluded that wind blowing over a 40 km wide and 1 m deep bay at the velocity of 2.2 m/s can generate shear stress of 0.2 Pa, which can often happen in Louisiana bays and estuaries. Xu et al. (2014) reported that the shear stress to generate tallest turbidity peaks was 0.6 Pa on Louisiana shelf based on in-situ GEMS measurements of 106 sediment cores, indicating a consolidated state of sediments which can be compared to our West Bay experimental cores that have been consolidated for more than 1 month (Figures 13-14). The critical shear stress results in GEMS measurements showed 2 and 4-month of consolidation were required to decrease significant amount of sediment resuspension.

4.1.2 Eroded mass

Same as the turbidity curve patterns, West Bay measurements show a clearer decreasing trend in eroded mass with increasing time of consolidation than that of Big Mar measurements (Figures 17-18). The decreasing in West Bay eroded mass with time indicates increased strengthening, which is likely to be the result of both self-weight consolidation and the bonds in the floc matrix. Relatively more sediment was eroded in West Bay 62.82 kg $m^{-3}$ measurements than that of West Bay 123.95 kg $m^{-3}$ measurements (Figure 18A-B) because of the proportional relationship between the critical shear stress and the sediment concentration.

On average about 0.16 kg $m^{-2}$ of sediment was eroded off the Louisiana shelf core tops when the 0.45 Pa shear stress was applied (Xu et al., 2014). This value was higher than that of all West Bay (the highest value was 0.15 kg $m^{-2}$) and most of Big Mar GEMS results in this experimental study (Figure 18). However, Xu et al. (2016) conducted the in-situ GEMS measurements in the field and found small eroded mass when 0.45 Pa of shear stress was applied (West Bay 0.08 kg $m^{-2}$, Big Mar 0.09 kg $m^{-2}$). Their eroded mass of West Bay is only smaller than that of 0.5-month experimental cores in our study. According to these data, the Louisiana shelf sediment was more mobile than our experimental sediment cores. The West Bay sediment cores collected and measured in the field by Xu et al. (2016) were more mobile than our experimental cores that have been consolidated for more than 1 month, but more consolidated than out 0.5-month experimental cores.

The erosional rate of sediment bed determines the local suspended sediment concentration and how much sediment can be transported to elsewhere. Erosional rate can be calculated from the eroded mass of sediment in suspension during an erosion measurement as a result of a larger bed shear stress than critical shear stress (Mehta, 2013). In Figure 18, the eroded mass of each measurement happened under the same conditions (water temperature, shear stresses, duration between each shear stress), so the eroded mass value can represent the erosion rate for each sediment core.

Studies have been done to demonstrate parameters that may influence erosion rates, and results showed that sediment bulk density, particle size distribution as well as mean particle size, mineralogy, organic content, and amounts and sizes of gas bubbles can contribute to erosion (Jepsen et al., 1997). In this study, 5 PSU of salinity was used for initial sediment suspension to form flocs. Low (60 kg $m^{-3}$) and high (120 kg $m^{-3}$) initial sediment concentrations were used to

measure erodibility. The turbidity and eroded mass of less organic-rich sediment (West Bay) decreased with increasing time of consolidation. Tangled organic matter in Big Mar sediment possibly makes it hard to predict sediment response to shear stress. But organic armoring would be eroded away first before the shear stress reach sediment beneath it. In this case, organic matter can protect sediment bed from erosion hence, increase sediment retention rate (Venier et al., 2012).

4.1.3 Organic mat

Organic matter in the water column was partly oxidized. As a result, the water appeared to be orange. The less dense organic matter settled slower than inorganic particles and deposited on top of sediment bed. After deposition, it was reduced in the upper part of the bed. After depletion of reducers, anaerobic fermentation occurred and some organic mats were produced at the sediment bed surface by bacteria during microbial processes, as well as some methane and carbon dioxide (Winterwerp and van Kesteren, 2004). These productions may be all entangled in the stability of the bed. They armored the surficial sediment from erosion during the first several shear stress stages. Once all mats were gone, sediment was eroded off the core top. The organic mats were generally lighter than sediment and could disperse under first several low shear stresses. After that, sediment beneath the mats was exposed to higher shear stresses. Sediment from Big Mar was finer than West Bay, thus was easier to be resuspended. Mariotti et al. (2014) conducted wave tank experiment and concluded that microbial aggregates can form wrinkle structures on a bed of bare sand with small orbital amplitude at the bed surface. The rounded-shape of organic mat groups on our sediment core tops was due to the lack of wave energy. However, it is likely that in an organic-rich semi-enclosed bay or estuary or lake with regularly

wind blowing would develop such organic mats on sediment bed and then influence the erosion processes.

### 4.2 Settling, Flocculation and Consolidation

In natural suspension, settling velocities of cohesive sediment aggregates are of the order of 0.01-10 mm/s and increase with sediment concentration up to 10 kg $m^{-3}$ due to flocculation. At a higher sediment concentration, the settling particles generate upward return flow, which affects its neighboring particle velocities. Three hours after consolidation tests started, coarse sediment suspended near the water surface captured in Figure 30 should be large-size but less-dense flocs. The return flow channels appear within the first few hours at the bottom of the settling column. Palermo and Thackston (1988) showed that greater initial sediment concentrations produce smaller void spaces and greater upward water velocity shears; as a result, the suspended sediment remains longer above the water-sediment interface. Flocs break-up should also be responsible for the slower settling (Mehta, 2013; Winterwerp and van Kesteren, 2004). Lutoclines often develop when sediment concentration exceeds 10 kg $m^{-3}$ (Ross and Mehta, 1991). The bulk density of sediment increases with depth and time due to the dewatering process and compaction. Trapping of water or bubble can cause local low density sometime (Jepsen et al., 1997).

All consolidation tests in terms of normalized sediment height versus time were compiled in Figure 26 with initial sediment concentration ranged from 10-120 kg $m^{-3}$ and two salinities (1 and 5 PSU). Various densities and sizes of flocs were distributed in the suspension and resulted in different settling velocities. Muste and Patel (1997) measured the suspended particle (250 μm for median diameter) velocities in a turbulent flow and found that their velocity fluctuations were smaller than for the liquid without a discernible influence on the liquid turbulence. Whitehouse

et al. (2000b) concluded that fluid suspended with fine-grained sediment in the marine environment can be treated as single-phase fluids and it is meaningful to define a bulk density like initial sediment concentration described in this study. Under still water conditions such as the settling column experiments in this study, once the sediment started to settle, the settling differences due to grain size, organic matter and salinity led to "multiple lutoclines" (Figure 21) , and this is particular true in low salinity (1 PSU) tests (Figure 20-21). However, sediment in the 5 PSU tests settled 'simultaneously' with one clear water-sediment interface. This phenomenon is probably related to ionic strength between flocs. In spite of the differential settling pattern of different salinity tests, both experiments had hindered settling and self-weight consolidation processes.

Regression analysis of $C_0$ and $t_{50}$ was conducted in Figure 28, displaying an exponential relationship between $C_0$ and $t_{50}$. West Bay and Big Mar sediment shared almost identical $t_{50}$ when salinity was 5 PSU, but varied in 1 PSU tests. This indicates that physical properties of sediment like grain size and organic matter content govern the settling process within a certain salinity range. When salinity was larger than a threshold value, probably between 1 to 5 PSU in this case, sediment settling rate does not change much.

### 4.3 Sediment Composition

Both West Bay and Big Mar sediment is consisted of silt, fine sand and clay grains mixed with detrital and organic matter. But West Bay possesses higher sandy sediment content. This is related to the physical location. West Bay is on the MRD which is under energetic physical oceanographic influence and is more prone to export mud to the GOM. The winnowing processes due to energetic waves and currents transported find sediments into the deeper sea. Xu et al. (2016) compiled a diverse of published sediment grain size data in not only the

Mississippi/Atchafalaya River Deltas but also Louisiana bays and estuaries, and found that silt is the largest fraction. The large fraction of silt should be taken into consideration in diversion design as grain size distribution can influence sediment bed erosion rate and particle settling velocity.

### 4.4 Sanford (2008) Model Response to the Experimental Data

Sanford (2008) erosion, deposition and consolidation model was calibrated and tested for the high initial concentration (120 kg $m^{-3}$) consolidation tests. The adjustable coefficient in Sanford (2008) is the consolidation rate $r_c$ ($d^{-1}$):

$$\frac{\partial \tau_c}{\partial t} = r_c(\tau_{ceq} - \tau_c)H(\tau_{ceq} - \tau_c) - r_s(\tau_{ceq} - \tau_{ceq}) \quad (4)$$

$$\frac{\partial \emptyset_s}{\partial t} = r_c(\emptyset_{seq} - \emptyset_s)H(\emptyset_{seq} - \emptyset_s) - r_s(\emptyset_{seq} - \emptyset_s - \emptyset_{seq}) \quad (5)$$

$H$ is the Heaviside step function, $r_c$ ($d^{-1}$) is the first-order consolidation rate, $r_s$ ($d^{-1}$) is the first-order swelling rate, which is 100 times slower than $r_c$ and was ignored in this study as zero due to the relatively short timescales, $\tau_c$ is critical stress (Pa), $\tau_{seq}$ is equilibrium profile of mud critical stress (Pa), $\emptyset_s$ is the general solids volume fraction and $\emptyset_{seq}$ is the equilibrium profile of mud solids volume fraction.

Sediment settling transferred from early settling stage to self-weight consolidation stage within the first 100 hours after the beginning of the experiment (Figure 26). Based on this and our experiment sampling time, the 97$^{th}$ hour after the beginning of the experiment was used as the transition from early settlement to self-weight consolidation. The experimental consolidation data from the 97$^{th}$ hour after the beginning of the experiment to the end was extracted and plotted in Excel. The coefficients (Table 3) for self-weight consolidation stage were determined by

exponential regression analysis of this part of the experimental consolidation data (>97h) in Excel and added to Sanford (2008) model to improve the prediction:

$$h = k_1 e^{-k_2 t} \quad (6)$$

Where $h$ is sediment bed height at time $t$; $k_1$ and $k_2$ are linear and exponential coefficients for self-weight consolidation, respectively. The method described by Sanford (2008) was used for the first 96 hours of settling after the beginning of the experiment. Equation 6 and coefficients that were determined by Excel exponential regression analysis were added to Sanford (2008) model to fit self-weight consolidation stage.

Table 3. Coefficients for self-weight consolidation stages in Figure 26, using Equation 6.

| Coefficient[a] | WB 1 PSU | WB 5 PSU | BM 1 PSU | BM 5 PSU |
|---|---|---|---|---|
| Init. Conc. (kg $m^{-3}$) | 119.70 | 120.23 | 123.23 | 122.38 |
| $k_1$ | 0.2290 | 0.2952 | 0.2770 | 0.3153 |
| $k_2$ | 0.0005 | 0.0003 | 0.0007 | 0.0010 |

[a] Definitions: $h$, sediment bed height at time $t$; $k_1$ and $k_2$, linear and exponential coefficient for sefl-weight consolidation, respectively.

Red dashed curves in Figure 26 are model predicting profiles illustrate the normalized sediment height versus consolidation time. Various consolidation rates $(r_c)$ were adjusted and those with the best fit to the experimental data were shown in Figure 26. Based on visual comparison, Sanford (2008) model fits the early settling stages for West Bay tests but not for Big Mar tests. The self-weight consolidation stages were well predicted by adding the coefficients that were determined from exponential regression analysis, which indicates that model using single exponential consolidation rate can only simulate either early settling or self-weight consolidation process, but not both. An equation including two exponential coefficients may represent both processes:

$$H_t = H_\infty + ae^{(-bt)} + ce^{(-dt)} \quad (7)$$

Where $H_t$ is sediment bed height measured at time *t*, $H_\infty$ is the asymptotic height after long time of self-weight consolidation, *a* and *b* are the linear and exponential coefficients for hindered settling in the first stage, and *c* and *d* are the linear and exponential coefficients for self-weight consolidation in the second stage, respectively. A similar but more complicated model can be found in the study of Toorman and Berlamont (1993). Once the coefficients can be determined according to different study sites and sediment properties, this method can be used to predict time-series consolidation to help engineering purpose or modeling calibration.

The Sanford model does not work well for any of Big Mar tests, which suggests that organic material influences the settling processes and should be taken into consideration for modeling in the future. Sanford (2008) model is computational efficient but lack of flocculation details.

**4.5 Implication for Coastal Restoration**

Cohesive sediment occupies large fraction in sediment-laden water and unconsolidated bed surface, both are important for natural and engineered sediment deposits in coastal area. Much effort has been made to sand, but not so much on mud, which is complex to understand and to put into practice. The sea level rise and subsidence rates have been studied using numerous methods for decades. Relative sea-level rise rates along coastal Louisiana (1.04 cm/yr) are about five to ten times the rate of eustatic sea-level rise, being a result of the world ocean expansion, climatic changes and wetland subsidence (Boesch et al., 1994). However, the consolidation rate of cohesive sediment in receiving basin has not been well understood yet. Neither does its resuspension response to wave/wind/current-induced shear stress. Results from this study are the fundamental knowledge that is urgently needed for further studies and

engineering designs for marsh creation and sediment diversion. From the results of this study, 2 and 4-month of consolidation are essential for cohesive sediment at low to high concentrations (e.g., 60 and 120 kg $m^{-3}$) to be strengthened enough to resist typical shear stress (0.2 Pa) in coastal Louisiana. Organic matter plays a large role on both sediment resuspension and consolidation. Salinity is also an important factor; it impacts cohesive sediment settling within small certain range which is site-specific, beyond that threshold the influence is not discernable. Coastal Louisiana has fresh, intermediate, brackish and salt marshes, and the salinity variations are important for vegetation and sediment dynamics, so it should be taken into consideration for dredging project design.

The present consolidation results show that further studies should extend the range of the salinity at a narrower interval. Interestingly, the studied results of Eisma et al. (1991) and Eisma (1991) suggested that the most important factors influencing floc size and character should be changes in turbulence and bottom shear. Addition of controlled-shear stress in the experiments (e.g., manmade waves) would improve our understanding of mud behaviors under the controls of forcings. In addition, it is worthwhile to study the effects of the mineral composition of sediment on its mechanical behavior. Different clay minerals have different chemical and physical properties. Knowing exactly the type of clay mineral would help improve our understanding on how the cohesive sediment component governs its behavior in flocculation and settling.

# CHAPTER 5. CONCLUSION

1) West Bay sediment has relatively low organic matter content and strengthens with time. Coupled consolidation and resuspension tests for initial concentration ($C_0$) at 60 kg $m^{-3}$ showed that the critical shear stress increased from 0.2 Pa after 2-month of consolidation to 0.45 Pa after 4-month of consolidation. The erodibility decreases with increasing time of consolidation. Cores formed with higher initial sediment concentration consolidate faster than lower initial sediment concentration cores.
2) When sediment grain size and experimental conditions (room temperature, same salinities) are similar, organic matter content plays a role on sediment erosional behaviors, which lead to a weak correlation between erodibility and time of consolidation for Big Mar resuspension tests.
3) West Bay and Big Mar sediment showed similar $t_{50}$ (time for sediment surface to reach half of its original height) for 5 PSU consolidation tests but smaller and different $t_{50}$ values for 1 PSU consolidation tests. Organic-rich sediment of Big Mar 1 PSU tests settled fastest. These results suggest that sediment settles faster at 1 PSU than at 5 PSU and organic content facilitates flocculation and governs sediment's settling behavior when salinity is low.
4) Low salinity consolidation tests have higher final sediment concentrations at the bottom and lower asymptotic sediment bed heights. When sediment sources, initial sediment concentrations and experimental temperatures are the same, salinity influences sediment's final consolidation state.
5) Silt is the dominant grain size in both West Bay and Big Mar. In both settling column and experimental cores, sediment shows a coarsening downward grain size distribution while

settling. In the settling column, however, coarser but less dense flocs may be suspended close to water surface.

6) Single exponential coefficient model (Sanford 2008) can only simulate either early settling or self-weight consolidation process, but not both. Involvement of organic material in sediment made it challenging to predict the settling behavior using this model.

## REFERENCES


Allison, M.A., Demas, C.R., Ebersole, B.A., Kleiss, B.A., Little, C.D., Meselhe, E.A., Powell, N.J., Pratt, T.C., Vosburg, B.M., 2012. A water and sediment budget for the lower Mississippi–Atchafalaya River in flood years 2008–2010: Implications for sediment discharge to the oceans and coastal restoration in Louisiana. Journal of Hydrology 432–433, 84-97.

Allison, M.A., Meselhe, E.A., 2010. The use of large water and sediment diversions in the lower Mississippi River (Louisiana) for coastal restoration. Journal of Hydrology 387, 346-360.

Baker, A., Henkel, T., Lopez, J., Boyd, E., 2011. Geomorphology and bald cypress resotration of the Caernarvon Delta near the Caernarvon Diversion, Southeast Louisiana. Lake Pontchartrain Basin Foundation, Coastal Sustainability Program.

Been, K., Sills, G.C., 1981. Self-weight consolidation of soft soils: an experimental and theoretical study. Géotechnique 31, 519-535.

Black, K., 1997. Microbiological factors contributing to erosion resistance in natural cohesive sediments. Cohesive Sediments, 231-244.

Blum, M.D., Roberts, H.H., 2009. Drowning of the Mississippi Delta due to insufficient sediment supply and global sea-level rise. Nature Geosci 2, 488-491.

Boesch, D.F., Josselyn, M.N., Mehta, A.J., Morris, J.T., Nuttle, W.K., Simenstad, C.A., Swift, D.J., 1994. Scientific assessment of coastal wetland loss, restoration and management in Louisiana. Journal of Coastal Research, i-103.

Burt, T.N., 1986. Field Settling Velocities of Estuary Muds, in: Mehta, A.J. (Ed.), Estuarine Cohesive Sediment Dynamics: Proceedings of a Workshop on Cohesive Sediment Dynamics with Special Reference to Physical Processes in Estuaries, Tampa, Florida, November 12–14, 1984. Springer New York, New York, NY, pp. 126-150.

Couvillion, B.R., Barras, J.A., Steyer, G.D., Sleavin, W., Fischer, M., Beck, H., Trahan, N., Griffin, B., Heckman, D., 2011. Land area change in coastal Louisiana from 1932 to 2010. U.S. Geological Survey Scientific Investigations Map 3164, scale 1:265,000, 12 p. pamphlet.

CPRA, 2012. Louisiana's Comprehensive Master Plan for a Sustainable Coast. Coastal Protection and Resotration Authority of Louisiana Baton Rouge, LA, USA.

Craft, C., Eugene Turner, R., Streever, B., 2002. Approaches to Coastal Wetland Restoration: Northern Gulf of Mexico. Restoration Ecology 10, 731-732.

Davies, H.C., 1982. The hurricane and its impact. By Robert H. Simpson and Herbert Riehl. Basil Blackwell, Publishers. 1981. Pp. 398, Figs. 152, Tables 36. $20.00. Quarterly Journal of the Royal Meteorological Society 108, 265-265.

Day, J.W., 2007. Restoration of the Mississippi Delta: Lessons from Hurricanes Katrina and Rita. Science 315, 1679-1684.

Day, J.W., Boesch, D.F., Clairain, E.J., Kemp, G.P., Laska, S.B., Mitsch, W.J., Orth, K., Mashriqui, H., Reed, D.J., Shabman, L., Simenstad, C.A., Streever, B.J., Twilley, R.R., Watson, C.C., Wells, J.T., Whigham, D.F., 2007. Restoration of the Mississippi Delta: Lessons from Hurricanes Katrina and Rita. Science 315, 1679-1684.

Dickhudt, P.J., Friedrichs, C.T., Sanford, L.P., 2011. Mud matrix solids fraction and bed erodibility in the York River estuary, USA, and other muddy environments. Continental Shelf Research 31, S3-S13.

Dickhudt, P.J., Friedrichs, C.T., Schaffner, L.C., Sanford, L.P., 2009. Spatial and temporal variation in cohesive sediment erodibility in the York River estuary, eastern USA: A biologically influenced equilibrium modified by seasonal deposition. Marine Geology 267, 128-140.

Dyer, K.R., 1989. Sediment processes in estuaries: Future research requirements. Journal of Geophysical Research: Oceans 94, 14327-14339.

Eisma, D., 1991. Particle size of suspended matter in estuaries. Geo-Marine Letters 11, 147-153.

Eisma, D., Bernard, P., Cadée, G.C., Ittekkot, V., Kalf, J., Laane, R., Martin, J.M., Mook, W.G., Van Put, A., Schuhmacher, T., 1991. Suspended-matter particle size in some west-European estuaries; part I: Particle-size distribution. Netherlands Journal of Sea Research 28, 193-214.

Folk, R.L., 1966. A REVIEW OF GRAIN-SIZE PARAMETERS. Sedimentology 6, 73-93.

Gust, G., Muller, V., 1997. Interfacial hydrodynamics and entrainment functions of currently used erosion devices, in: Burt, N., Parker, R., Watts, J. (Eds.), Cohesive Sediments, Wallingford, UK, pp. 149-174.

Heiri, O., Lotter, A., Lemcke, G., 2001. Loss on ignition as a method for estimating organic and carbonate content in sediments: reproducibility and comparability of results. Journal of Paleolimnology 25, 101-110.

Jackson, J.B.C., Kirby, M.X., Berger, W.H., Bjorndal, K.A., Botsford, L.W., Bourque, B.J., Bradbury, R.H., Cooke, R., Erlandson, J., Estes, J.A., Hughes, T.P., Kidwell, S., Lange, C.B., Lenihan, H.S., Pandolfi, J.M., Peterson, C.H., Steneck, R.S., Tegner, M.J., Warner, R.R., 2001. Historical Overfishing and the Recent Collapse of Coastal Ecosystems. Science 293, 629-637.

Jepsen, R., Roberts, J., Lick, W., 1997. Effects of bulk density on sediment erosion rates. Water, Air, and Soil Pollution 99, 21-31.

Khalil, S.M., Raynie, R.C., Muhammad, Z., Killebrew, C., 2011. Overview of coastal restoration in Louisiana. Journal of the American Shore & Beach Preservation Association 79, 4-11.

Kineke, G.C., Sternberg, R.W., Trowbridge, J.H., Geyer, W.R., 1996. Fluid-mud processes on the Amazon continental shelf. Continental Shelf Research 16, 667-696.

Kolker, A.S., Miner, M.D., Weathers, H.D., 2012. Depositional dynamics in a river diversion receiving basin: The case of the West Bay Mississippi River Diversion. Estuarine, Coastal and Shelf Science 106, 1-12.

Krone, R.B., 1972. A field study of flocculation as a factor in estuarial shoaling processes, Tidal Hydraulics, Technical bulletin U.S Army Corps of Engineering, Comm.

Lane, R., Day, J., Thibodeaux, B., 1999. Water quality analysis of a freshwater diversion at Caernarvon, Louisiana. Estuaries 22, 327-336.

Law, B.A., Hill, P.S., Milligan, T.G., Curran, K.J., Wiberg, P.L., Wheatcroft, R.A., 2008. Size sorting of fine-grained sediments during erosion: Results from the western Gulf of Lions. Continental Shelf Research 28, 1935-1946.

Lo, E., Bentley, S., Sr., Xu, K., 2014. Experimental study of cohesive sediment consolidation and resuspension identifies approaches for coastal restoration: Lake Lery, Louisiana. Geo-Marine Letters 34, 499-509.

Lopez, J.A., Henkel, T.K., Moshogianis, A.M., Baker, A.D., Boyd, E.C., Hillmann, E.R., Connor, P.F., Baker, D.B., 2014. Examination of Deltaic Processes of Mississippi River Outlets - Caernarvon Delta and Bohemia Spillway in Southeastern Louisiana. Gulf Coast Association of Geological Sciences Transactions 3, 79–93.

Maa, J.P.Y., Sanford, L., Halka, J.P., 1998. Sediment resuspension characteristics in Baltimore Harbor, Maryland. Marine Geology 146, 137-145.

Mariotti, G., Fagherazzi, S., 2013. Critical width of tidal flats triggers marsh collapse in the absence of sea-level rise. Proceedings of the National Academy of Sciences 110, 5353-5356.

Mariotti, G., Pruss, S.B., Perron, J.T., Bosak, T., 2014. Microbial shaping of sedimentary wrinkle structures. Nature Geosci 7, 736-740.

McAnally, W.H., Friedrichs, C., Hamilton, D., Hayter, E., Shrestha, P., Rodriguez, H., Sheremet, A., Teeter, A., 2007. Management of Fluid Mud in Estuaries, Bays, and Lakes. I: Present State of Understanding on Character and Behavior. Journal of Hydraulic Engineering 133, 9-22.

Mehta, A.J., 2013. Characterization of Cohesive Sediment Properties and Transport Processes in Estuaries, Estuarine Cohesive Sediment Dynamics. Springer-Verlag, pp. 290-325.

Mickey, R., Xu, K., Libes, S., Hill, J., 2015. Sediment texture, erodibility, and composition in the Northern Gulf of Mexico and their potential impacts on hypoxia formation. Ocean Dynamics 65, 269-285.

Migniot, C., 1968. A study of the physical properties of various very fine sediments and their behaviour under hydrodynamic action La Houille Blanche 23, 591-620.

Morton, R.A., Bernier, J.C., Barras, J.A., 2006. Evidence of regional subsidence and associated interior wetland loss induced by hydrocarbon production, Gulf Coast region, USA. Environ. Geol. 50, 261-274.

Mulsow, S., Boudreau, B.P., Smith, J.A., 1998. Bioturbation and porosity gradients. Limnology and Oceanography 43, 1-9.

Muste, M., Patel, V.C., 1997. Velocity Profiles for Particles and Liquid in Open-Channel Flow with Suspended Sediment. Journal of Hydraulic Engineering 123, 742-751.

Nittrouer, J.A., Allison, M.A., Campanella, R., 2008. Bedform transport rates for the lowermost Mississippi River. Journal of Geophysical Research: Earth Surface 113, n/a-n/a.

Nittrouer, J.A., Best, J.L., Brantley, C., Cash, R.W., Czapiga, M., Kumar, P., Parker, G., 2012. Mitigating land loss in coastal Louisiana by controlled diversion of Mississippi River sand. Nature Geosci 5, 534-537.

Palermo, M., Thackston, E., 1988. Flocculent Settling Above Zone Settling Interface. Journal of Environmental Engineering 114, 770-783.

Paola, C., Twilley, R.R., Edmonds, D.A., Kim, W., Mohrig, D., Parker, G., Viparelli, E., Voller, V.R., 2011. Natural Processes in Delta Restoration: Application to the Mississippi Delta. Annual Review of Marine Science 3, 67-91.

Parchure, T., Mehta, A., 1985. Erosion of Soft Cohesive Sediment Deposits. Journal of Hydraulic Engineering 111, 1308-1326.

Reed, D.J., 2002. Sea-level rise and coastal marsh sustainability: geological and ecological factors in the Mississippi delta plain. Geomorphology 48, 233-243.

Rinehimer, J.P., Harris, C.K., Sherwood, C.R., Sanford, L.P., 2007. Estimating Cohesive Sediment Erosion and Consolidation in a Muddy, Tidally-Dominated Environment: Model Behavior and Sensitivity, Estuarine and Coastal Modeling (2007), pp. 819-838.

Roberts, J., Jepsen, R., Gotthard, D., Lick, W., 1998. Effects of Particle Size and Bulk Density on Erosion of Quartz Particles. Journal of Hydraulic Engineering 124, 1261-1267.

Ross, M.A., Mehta, A.J., 1991. Fluidization of Soft Estuarine Mud by Waves, in: Bennett, R.H., Bryant, W.R., Hulbert, M.H., Chiou, W.A., Faas, R.W., Kasprowicz, J., Li, H., Lomenick, T., O'Brien, N.R., Pamukcu, S., Smart, P., Weaver, C.E., Yamamoto, T. (Eds.), Microstructure of Fine-Grained Sediments: From Mud to Shale. Springer New York, New York, NY, pp. 185-191.

Sanford, L.P., 2008. Modeling a dynamically varying mixed sediment bed with erosion, deposition, bioturbation, consolidation, and armoring. Computers & Geosciences 34, 1263-1283.

Sanford, L.P., Maa, J.P.Y., 2001. A unified erosion formulation for fine sediments. Marine Geology 179, 9-23.

Shea, P., Karen, E.R., 1990. Relative Sea-Level Rise in Louisiana and the Gulf of Mexico: 1908-1988. Journal of Coastal Research 6, 323-342.

Smith, J.E., Bentley, S.J., Snedden, G.A., White, C., 2015. What Role do Hurricanes Play in Sediment Delivery to Subsiding River Deltas? Scientific Reports 5, 17582.

Stanley, D.J., Warne, A.G., 1998. Nile Delta in Its Destruction Phase. Journal of Coastal Research 14, 795-825.

Stevens, A.W., Wheatcroft, R.A., Wiberg, P.L., 2007. Seabed properties and sediment erodibility along the western Adriatic margin, Italy. Continental Shelf Research 27, 400-416.

Swarzenski, C.M., Doyle, T.W., Fry, B., Hargis, T.G., 2008. Biogeochemical response of organic-rich freshwater marshes in the Louisiana delta plain to chronic river water influx. Biogeochemistry 90, 49-63.

Syvitski, J.P.M., Kettner, A.J., Overeem, I., Hutton, E.W.H., Hannon, M.T., Brakenridge, G.R., Day, J., Vorosmarty, C., Saito, Y., Giosan, L., Nicholls, R.J., 2009. Sinking deltas due to human activities. Nature Geosci 2, 681-686.

Syvitski, J.P.M., Saito, Y., 2007. Morphodynamics of deltas under the influence of humans. Global and Planetary Change 57, 261-282.

Syvitski, J.P.M., Vörösmarty, C.J., Kettner, A.J., Green, P., 2005. Impact of Humans on the Flux of Terrestrial Sediment to the Global Coastal Ocean. Science 308, 376-380.

Temmerman, S., Kirwan, M.L., 2015. Building land with a rising sea. Science 349, 588-589.

Tessler, Z.D., Vörösmarty, C.J., Grossberg, M., Gladkova, I., Aizenman, H., Syvitski, J.P.M., Foufoula-Georgiou, E., 2015. Profiling risk and sustainability in coastal deltas of the world. Science 349, 638-643.

Thorn, M., 1987. Coastal and estuarine sediment dynamics by K.R. Dyer. Wiley, Chichester, 1986. No. of pages: 358. Price: ±36.00 (Hardback). Geological Journal 22, 169-169.

Toorman, E.A., Berlamont, J.E., 1993. Mathematical Modeling of Cohesive Sediment Settling and Consolidation, Nearshore and Estuarine Cohesive Sediment Transport. American Geophysical Union, pp. 167-184.

Tornqvist, T.E., 1996. A revised chronology for Mississippi River subdeltas. Science 273, 1693-1696.

Tornqvist, T.E., Wallace, D.J., Storms, J.E.A., Wallinga, J., van Dam, R.L., Blaauw, M., Derksen, M.S., Klerks, C.J.W., Meijneken, C., Snijders, E.M.A., 2008. Mississippi Delta subsidence primarily caused by compaction of Holocene strata. Nature Geosci 1, 173-176.

Turner, R.E., 1997. Wetland loss in the Northern Gulf of Mexico: Multiple working hypotheses. Estuaries 20, 1-13.

Turner, R.E., Baustian, J.J., Swenson, E.M., Spicer, J.S., 2006. Wetland Sedimentation from Hurricanes Katrina and Rita. Science 314, 449-452.

Turner, T., 1996. Fundamentals of Hydraulic Dredging. ASCE Press.

Venier, C., Figueiredo da Silva, J., McLelland, S.J., Duck, R.W., Lanzoni, S., 2012. Experimental investigation of the impact of macroalgal mats on flow dynamics and sediment stability in shallow tidal areas. Estuarine, Coastal and Shelf Science 112, 52-60.

Wells, J.T., Coleman, J.M., 1987. Wetland loss and the subdelta life cycle. Estuarine, Coastal and Shelf Science 25, 111-125.

Whitehouse, R., Soulsby, R., Roberts, W., Mitchener, H., 2000a. Dynamics of estuarine muds: a manual for practical applications. Thomas Telford, London.

Whitehouse, R.J.S., Soulsby, R.L., Roberts, W., Mitchener, H.J., 2000b. Dynamics of Estuarine Muds, A Manual for Practical Applications. Thomas Telford, London.

Wiberg, P.L., Smith, J.D., 1987. Calculations of the critical shear stress for motion of uniform and heterogeneous sediments. Water Resources Research 23, 1471-1480.

Winterwerp, J.C., van Kesteren, W.G.M., 2004. Introduction to the Physics of Cohesive Sediment in the Marine Environment. Elsevier.

Xu, K., Bentley, S., Robichaux, P., Sha, X., Yang, H., 2016. Implications of Texture and Erodibility for Sediment Retention in Receiving Basins of Coastal Louisiana Diversions. Water 8, 26.

Xu, K., Corbett, D.R., Walsh, J.P., Young, D., Briggs, K.B., Cartwright, G.M., Friedrichs, C.T., Harris, C.K., Mickey, R.C., Mitra, S., 2014. Seabed erodibility variations on the Louisiana continental shelf before and after the 2011 Mississippi River flood. Estuarine, Coastal and Shelf Science 149, 283-293.

# APPENDIX

## Original Sanford (2008) model Matlab files and improvements

The original MATLAB script package of Sanford (2008) model includes 6 .m files and 2 Excel files of published experimental data. The .m file that called 'TBConsolCompare' was used and improved in this study. This .m file has 106 lines in total. No changes have been made to the original code except the initial condition setups as mentioned in methods and discussion in this thesis and the addition of the Equation 6 at the end of the code as below:

Line 1: k=find(abs(t-4)<0.001);

Line 2: zt1=1.858-z(1,1:k);

Line 3: znorm1=zt1/1.858;

Line 4: kt=find(abs(t-t(end))<0.001);

Line 5: zt2=0.2771*exp(-0.0007*24.*t((k+1):kt));

Line 6: znorm2=zt2/1.858;

Line 7: znorm=[znorm1 zt2];

The first two lines here extracts the sediment height values of the early settling stage (<97h) from the results that were calculated in the original code. The third line calculates the normalized sediment height values using the sediment height values just extracted and the initial sediment height for early settling stage (<97h). The fourth line defines the self-weight consolidation time, which started from the 97$^{th}$ hours after the beginning of the experiment. The fifth line is the Equation 6 ($h = k_1 e^{-k_2 t}$) with the coefficients for Big Mar 1 PSU 123.23 kg m$^{-3}$ test ($k_1$=0.2771, $k_2$=0.0007, $t$>97). The sixth line calculates the normalized sediment height for self-weight consolidation stage (>97h). The seventh line merges the two stages into one matrix.

Then, the normalized sediment height values of the whole settling process were extracted and plotted in SigmaPlot.

# VITA

Xiaoyu Sha was born on March 15, 1993. She comes from one of the most amazing grasslands in the world, Hunlunbeier, China. There she realized the best colors and the prettiest things are all from nature. She has seen horses running, sheep grazing and shepherd singing on the grassland. She knew the meaning of freedom. She also has dreams.

She graduated from China University of Petroleum (East China) in 2014 with Geology and English double bachelor degrees. During that period, she was involved in several geological projects and experiments. She got the first chance to study abroad supported by China Scholarship Council (CSC) when she was a senior undergraduate student. She went to Missouri University of Science and Technology, Rolla, Missouri, as a visiting student to complete her undergraduate thesis project about unconventional oil and gas. After graduation, Xiaoyu received an offer from the Department of Oceanography and Coastal Sciences at Louisiana State University to work on the restoration project, under the co-supervision of Drs. Kevin Xu and Sam Bentley. Xiaoyu will graduate in August of 2016 with the degree of Master of Science. She is ready to embrace the unknown world.